

Late Paleozoic glacial to postglacial stratigraphic evolution of the Rio do Sul depocenter, Itararé and Guatá groups, Pennsylvanian-Cisuralian, southern Brazil

Danielle Cristine Buzatto Schemiko^{1*} , Fernando Farias Vesely¹ ,
Mérolyn Camila Naves de Lima Rodrigues¹ 

Abstract

The transition from the Late Paleozoic Ice Age (LPIA) to fully postglacial conditions in SW Gondwana is under increasing discussion due to either the radiometric ages of its boundary or the stratigraphic nature of this transition. The record of this transition in the Paraná Basin is found in the glacial and glacially influenced deposits of the upper Mafra and Rio do Sul Formations (upper Itararé Group) and postglacial strata of the Rio Bonito Formation (Guatá Group). Here we address the depositional architecture and stratigraphic evolution of these deposits in the Rio do Sul depocenter, eastern Paraná Basin, Brazil, the main area of subsidence in the basin during this transition in Pennsylvanian-Cisuralian time, bringing an opportunity to examine the characteristics of glacial to postglacial transition. Analyses of facies, stratigraphic logs, stratigraphic correlations, and paleocurrent dispersal trends allowed us to define three evolutionary stages. The first stage registers glacial advance from the south-southwest represented by an erosive surface and subglacial tillites. Gravitational deposits covered the tillites in response to ice retreat (upper Mafra Formation), and the Lontras Shales (lower Rio do Sul Formation) correspond to the marine maximum flooding. The second stage comprises co-genetic deepwater (Rio do Sul Formation) to shallow (Rio Bonito Formation, Triunfo Member) progradational deposits after the Lontras Shale maximum flooding. Paleocurrent data and glacially related features point to glaciated source areas located to the NE, E, and SE for the Rio do Sul depocenter during this stage. The third stage corresponds to retrogradational stacking pattern upon a fluvial subaerial unconformity (incised valley), starting with fluvio-deltaic beds (Triunfo Member), followed by fine-grained deposits of the Paraguaçu Member of Rio Bonito Formation. No features related to glacial influence characterize this third stage. As previously suggested, tectonic uplift likely drove the additional NE source and created the space that allowed the transitional contact between Rio do Sul and Rio Bonito formations in the Rio do Sul depocenter.

KEYWORDS: Late Paleozoic Ice Age; Gondwanan palaeogeography; glacially influenced deposits; co-genetic deepwater to shallow deposits.

INTRODUCTION

The Rio do Sul depocenter was the main subsiding area during the Pennsylvanian-Permian transition of the Paraná Basin, filled mainly by glacio-influenced, deep-marine deposits of the Rio do Sul Formation (upper Itararé Group, Ramos 1967, Northfleet *et al.* 1969, Medeiros and Thomaz Filho 1973, Schneider *et al.* 1974, Castro 1980, 1991, Eyles *et al.* 1993). Its name refers to where these deposits can reach their maximum thickness (about 330 m, Schneider *et al.* 1974) in the Rio do Sul locality, Santa Catarina State, southern Brazil. Those deep-marine deposits are superposed by fluvio-deltaic strata (Rio Bonito Formation), composing one of the outstanding intervals of the basin regarding mineral and energy potential (França and Potter 1988). The Itararé

Group holds gas reservoirs (Campos *et al.* 1998), and the Rio Bonito Formation hosts almost all the coal deposits in Brazil (Milani *et al.* 2007).

It has been widely reported the likely genetic link between the uppermost strata of the Itararé Group (Rio do Sul Formation) and the lowermost interval of the Rio Bonito Formation (Triunfo Member) in Santa Catarina State (e.g., Medeiros and Thomaz Filho 1973, Castro 1980, Schneider *et al.* 1974, Canuto 1993, Santos *et al.* 1996, D'Ávila 2009, Schemiko *et al.* 2019), configuring an up to 500-m-thick succession. The Rio do Sul Formation stands out due to gravitational flow deposits, such as subaqueous slumps and slides, debris flows, and turbidities, possibly developed on a paleogradient to the west-northwest (Medeiros and Thomaz Filho 1973, Castro 1980, 1991). Likewise, Medeiros and Thomaz Filho (1973) recognized deltaic and coastal tide-influenced deposits in the Rio Bonito Formation. The paleogeographic model proposed by these authors points to the existence of a source area to the east, and the development of deltas toward the west, in similar paleoflow directions to the lowermost gravitational deposits.

Both tectonics and the presence of glaciers could be the reason for the high rate of subsidence and the somewhat deep sea during the sedimentation of the uppermost Itararé Group

¹Programa de Pós-Graduação em Geologia, Departamento de Geologia, Universidade Federal do Paraná – Curitiba (PR), Brazil. E-mails: danielleschemiko@gmail.com, vesely@ufpr.br, merolyn.cnlr@gmail.com, merolyn.rodrigues@ufpr.br

*Corresponding author.



in the Rio do Sul area. Previous works suggested a likely tectonic uplift of the northern portion of the Paraná Basin during the final stage of the Itararé Group deposition, leading to the displacement of the main depocenters toward the south. It configured the so-called embayment, sub-basin, or depocenter of Rio do Sul (Ramos 1967, Northfleet *et al.* 1969, Medeiros and Thomaz Filho 1973, Santos 1987, Canuto 1993, Santos *et al.* 1996). Therefore, the basement structures might have compartmentalized the basin, delimited depocenters, and controlled the emplacement of paleoslopes (e.g., Castro 1991, Rostirolla *et al.* 2000, Riccomini *et al.* 2005).

This study is a complement to the previous work by Schemiko *et al.* (2019) that describes the genetic relationship between glacially influenced deepwater (Rio do Sul Formation) and fluvio-deltaic (Rio Bonito Formation) deposits within the same depositional tract in the northeastern region of Rio do Sul depocenter (Santa Catarina State), showing a transitional contact. Nevertheless, the transition between the upper Itararé Group and Rio Bonito Formation occurs through an abrupt contact in the northern part of the basin (e.g., Paraná State, Zacharias and Assine 2005, Mottin *et al.* 2018). Thus, this article aimed at a detailed analysis of the depositional framework of the Rio do Sul depocenter to understand the stratigraphic evolution of the Pennsylvanian-Permian transition in the southern sector of Paraná Basin (southern Gondwana). The study area consists of an elongated polygon between Alfredo Wagner (SE) and Witmarsum (NW) localities. The main methods employed include the construction of vertical stratigraphic profiles, recognition of the facies and facies associations, definition of vertical depositional trends and the key surfaces, correlation of outcrop and subsurface data, and paleocurrent analysis.

GEOLOGICAL SETTING

The Paraná Basin is a large intraplate basin covering up to 1,600,000 km² of central-southern of South America. The upper Paleozoic succession is the thickest of the Paraná Basin and embraces stratigraphic units deposited in marine to continental environments that compose the Itararé and Guatá groups. The study interval encompasses the glacially related strata of the upper Itararé Group (Rio do Sul Formation) and the postglacial sediments of the lower Guatá Group (coal-bearing Rio Bonito Formation).

Successive deglaciation phases of the Late Paleozoic Ice Age (LPIA) (Glacial I, II, and III; Isbell *et al.* 2003, López-Gamundí and Buatois 2010) across the Paraná Basin led to the deposition of strata set over 1,300-m thick composed overall of proglacial deposits of the Itararé Group (França and Potter 1988, Vesely and Assine 2006), corresponding to different formal stratigraphic units. Schneider *et al.* (1974), based on outcrop studies along the eastern portion of the Paraná Basin, divided the Itararé Group into the Campo do Tenente, Mafra, and Rio do Sul formations, where the Lontras Shale is placed in the base of Rio do Sul Formation (Fig. 1). After that, França and Potter (1988), based on subsurface data, subdivided it into Lagoa Azul, Campo Mourão,

and Taciba formations. The upper Itararé Group can show a transitional (e.g., Medeiros and Thomaz Filho 1973, Castro 1991, Castro *et al.* 2004, Schemiko *et al.* 2019) or abrupt contact (e.g., Vesely and Assine 2006, Mottin *et al.* 2018, Valdez Buso *et al.* 2019) with postglacial deposits of the Rio Bonito Formation of the Guatá Group. Schneider *et al.* (1974) also proposed the distinction between the units that make up the Guatá Group comprising the Rio Bonito (bottom) and Palermo (top) formations. In addition, they proposed the subdivision of the Rio Bonito Formation into Triunfo, Paraguaçu, and Siderópolis members (Fig. 1).

According to a detailed sequence stratigraphic study in the Rio Grande do Sul and southern Santa Catarina states, the upper Itararé Group and the entire Guatá Group embrace three third-order depositional sequences (Holz *et al.* 2006, 2010). The study interval is correlated to the first two sequences (Fig. 1). The basal sequence corresponds to the upper Itararé Group and includes a third-order sequence boundary (SB1) at the base, usually related to the crystalline basement, while the second third-order sequence boundary (SB2) delineates the boundary between glacially influenced deposits of Rio do Sul Formation and fluvial deposits of Triunfo Member (LST2). It grades upward to the offshore mudstones of Paraguaçu Member (TST2 and MFS2). The SB3, in turn, separates the upper Paraguaçu Member (HST2) from the fluvial to shallow-marine deposits of Siderópolis Member (LTS3), where the fine-grained deposits of Palermo Formation are the subsequent widespread transgression.

According to Iannuzzi (2010, Fig. 1), the proper interpretation of the sequence analysis of the Rio Bonito Formation facilitated the positioning of the coal seams and their absolute ages at the appropriate stratigraphic level, supporting the dating of the glacial-postglacial boundary of the Paraná Basin. In this context, the demise of the Ice Age in Paraná Basin, long ascribed to be Early Permian, is currently considered Pennsylvanian-Cisuralian. An essential contribution to the age positioning of the Itararé-Guatá contact was provided first by Cagliari *et al.* (2014) and corroborated by Cagliari *et al.* (2016) and Griffis *et al.* (2018, 2019). It is also supported by the new palynostratigraphic revision by Souza *et al.* (2021).

Although the Itararé Group seems to be restricted to the Carboniferous, the transition between Itararé Group and Rio Bonito Formation still belongs to the same palynozone (*Vittatina costabilis* Zone — VcZ), ranging from Gzhelian-Artinskian (Souza *et al.* 2021). It attests that there is no significant time gap or paleoecological changes for Itararé-Rio Bonito as previously reported (Daemon and Quadros 1970, Souza *et al.* 1999, Souza and Marques-Toigo 2005, Souza 2006, Mori *et al.* 2012, Mottin *et al.* 2018). Thus, the glacial-postglacial genetic criterion should not be used to delineate the lithostratigraphic boundary (e.g., Vesely 2006), particularly in the southern Brazilian states (Daemon and Quadros 1970).

The somewhat deepwater setting of the upper Itararé Group in the Santa Catarina State has been described as an embayment, a depocenter, or a sub-basin of the Rio do Sul (Santos 1987, Canuto 1993, Santos *et al.* 1996). The last deglacial event of the Rio do Sul Formation in this area has a

continuous deposition evolution with the lower Rio Bonito Formation by means of the relationship between deepwater systems, under the glacial influence, and the deltaic deposits in the same depositional tract (Schemiko *et al.* 2019). It can also be verified through transport patterns. The uppermost strata of Itararé Group show paleoflows to the NW, NNE, and SW (e.g., Castro 1980, 1991, D'Ávila and Paim 2003, Puigdomenech *et al.* 2014, Aquino *et al.* 2016, Fallgatter and Paim 2017), suggesting a paleogradient dipping to the west-northwest. The Rio Bonito Formation, in turn, had fluvio-deltaic systems prograding mainly to the west (Medeiros and Thomaz Filho 1973, Castro 1991). In this context, Castro (1980, 1991) reported scattered dropstones in the Rio Bonito Formation, indicating a relatively cold climate also during its deposition. However, in the northern portion of the basin (e.g., Paraná State), the contact between the upper Itararé Group and Rio Bonito Formation takes place through a discordant surface characterized by the presence of incised valleys developed on top of the diamictite-bearing units of the upper Itararé Group (Zacharias and Assine 2005, Mottin *et al.* 2018) and filled by essentially postglacial deposits. Even so, the paleocurrents of both units are toward the southwest in this region.

METHODS AND KEY DEFINITIONS

This study is based on an investigation of outcrops in the eastern border of Paraná Basin in southeastern Santa Catarina State, southern Brazil. The stratigraphic architecture was described in detail in the northern part of the study area (Witmarsum-Presidente Getúlio localities, Schemiko *et al.* 2019) and regionally recognized (Fig. 2) through stratigraphic and facies analysis of about 190 outcrops (Appendix 1) in road cuts, quarries, and natural exposures. Facies were distinguished according to Miall (1978) and Eyles *et al.* (1983).

Vertical logs and subsurface data were correlated to analyze the spatial distribution of facies associations and the vertical trends. It was integrated with the paleocurrent data to establish the paleogeographic models, including the representation of depositional environments and sediment transport patterns. Well data are from CPRM (Brazilian Geological Survey) and Petrobras, drilled during coal and oil exploration campaigns. The wells used in the correlations are 1-GO-1-SC, 2-AL-1-SC, 1-RCH-1-SC, 1-TP-3-SC, 2-TG-1-SC, 1-MB-1-SC, 1-BN-1-SC, and 1-PA-1-SC from Petrobras and 7-RL-4-SC from CPRM (Figs. 3 and 4).

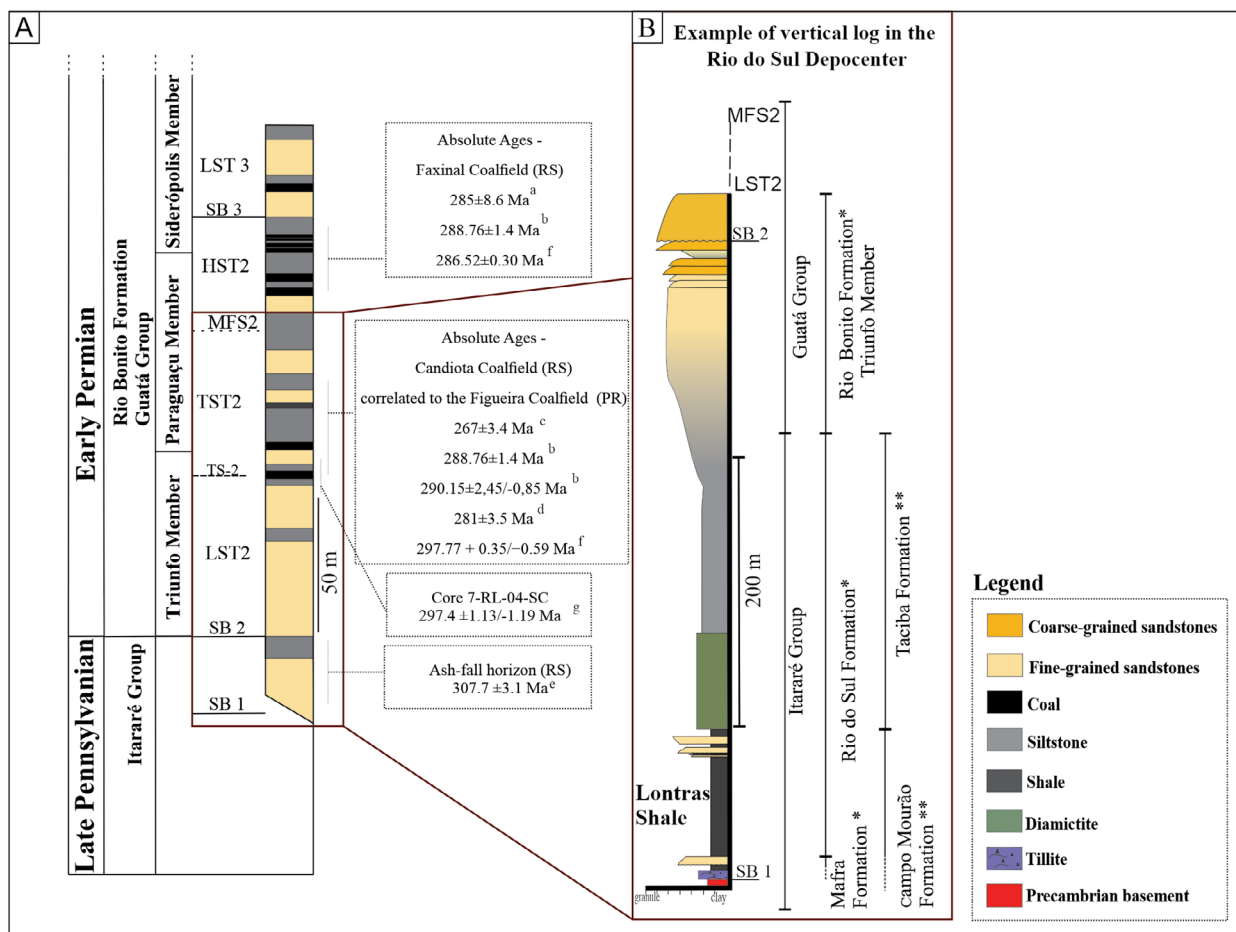


Figure 1. (A) Stratigraphic scheme of the Paraná Basin showing the study interval, embracing the upper Itararé Group and the lower Rio Bonito Formation (modified from Iannuzzi 2010 after Holz *et al.* 2010); (B) Emphasis on the interval selected for the study. Vertical log from Schemiko *et al.* (2019). Note the absolute ages of the Rio Bonito Formation coal deposits, especially those related to transgressive systems tracts, at the base of the Paraguçu Member. (1: a Guerra-Sommer *et al.* 2008a; b Guerra-Sommer *et al.* 2008b; c Matos *et al.* 2000, 2001; d Mori *et al.* 2012; e Cagliari *et al.* 2016; f Griffis *et al.* 2018; and g Griffis *et al.* 2019. For further absolute age summaries, see Valdez Buso *et al.* 2020, Souza *et al.* 2021, and Griffis *et al.* 2021. 2: *Schneider *et al.* 1974; and **França and Potter 1988).

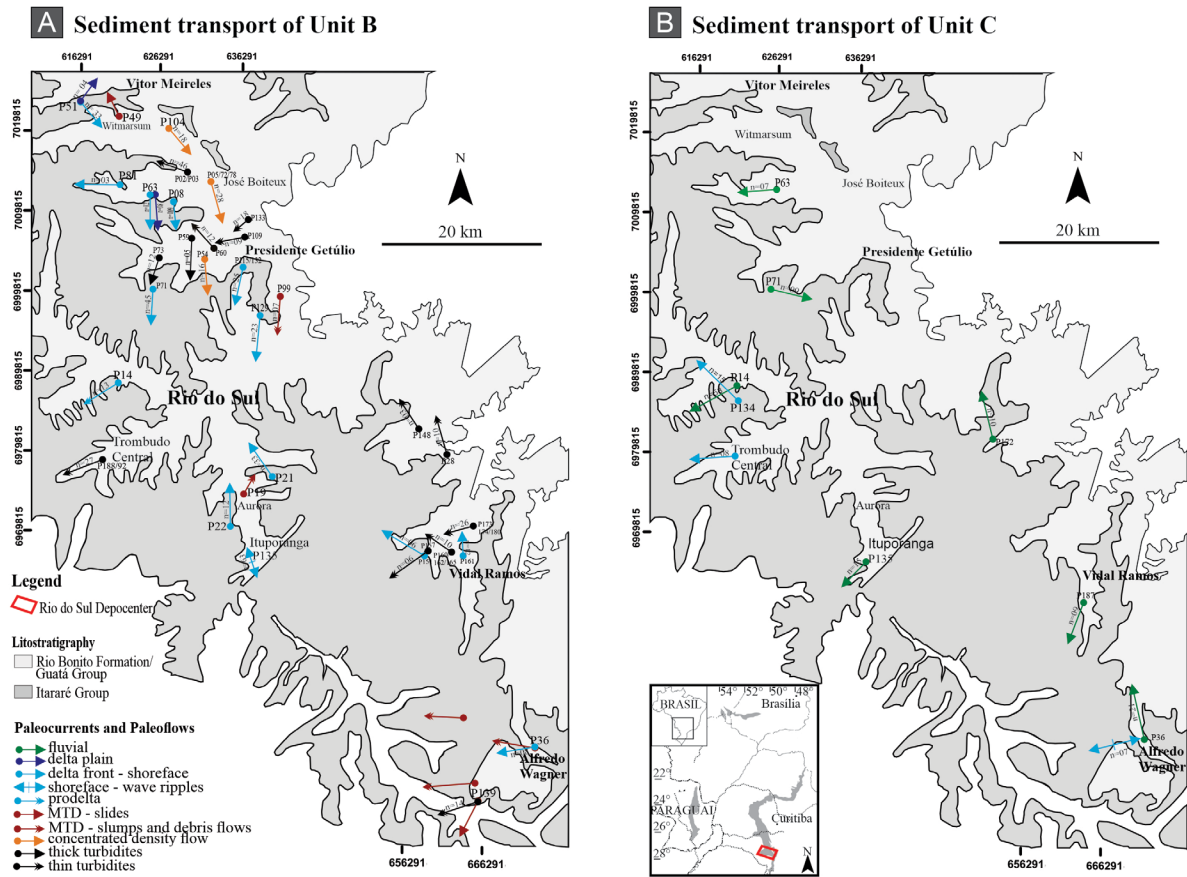


Figure 2. Location of the study area, between Alfredo Wagner (SE) and Witmarsum (NW) localities in Santa Catarina State, southern Brazil, with the arrangement of the paleocurrent readings of facies associations within (A) Units B and (B) Unit C. The sediment transport concerning the deposits of Unit A is documented by Aquino *et al.* (2016) and Fallgatter and Paim (2017), with main paleocurrents toward the northwest. The paleoflows directions of mass transport deposits are from Rodrigues *et al.* (2021), except for those from the P99 locality that was documented in Schemiko *et al.* (2019).

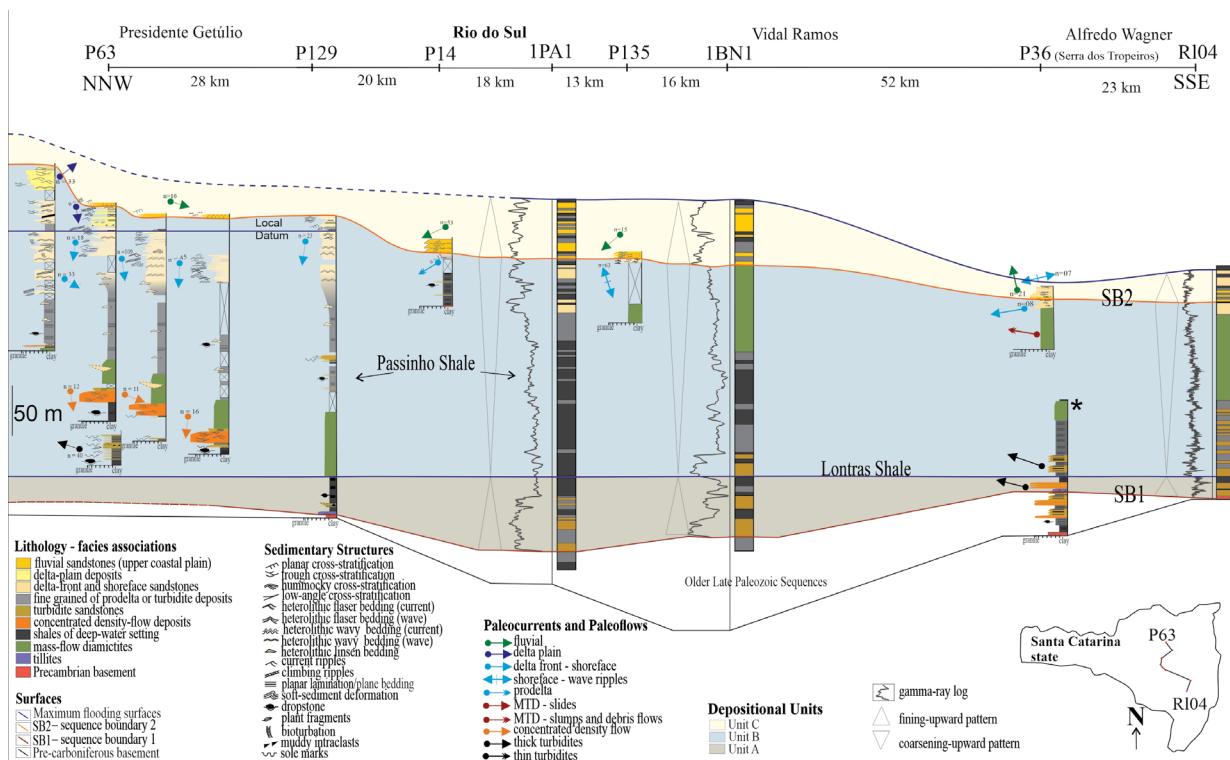


Figure 3. Stratigraphic framework of the Rio do Sul depocenter (Pennsylvanian-Permian of the Paraná Basin), showing the spatial distribution of the Units A, B, and C in an NWW-SSE correlation and covering up to 70 km long. Notice the convergence of paleocurrents and changes in the thickness of Passinho and Lontras Shales toward Rio do Sul locality. The asterisk corresponds to data from Fallgatter and Paim (2017).

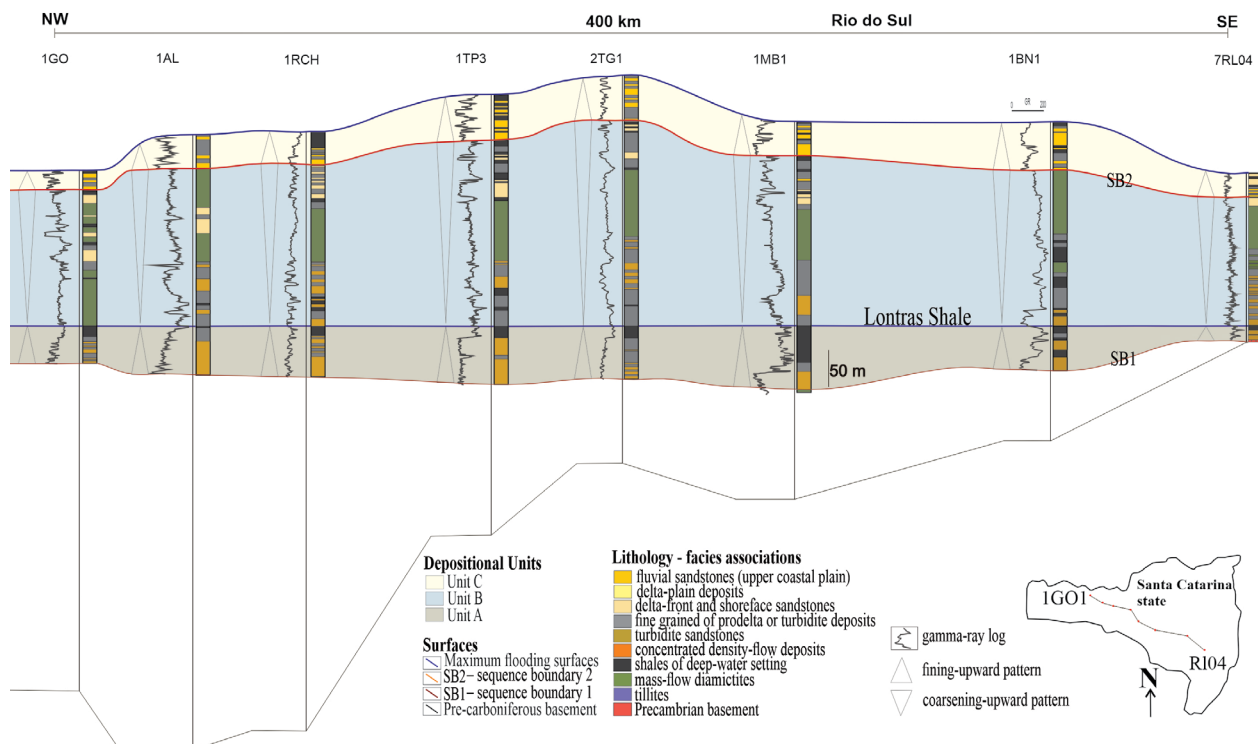


Figure 4. Stratigraphic framework of the Rio do Sul depocenter (Pennsylvanian-Permian of the Paraná Basin), showing the spatial distribution of the Units A, B, and C in an NW-SE correlation and covering up to 400 km long. It suggests the regional expression of the recognized units that compose the Rio do Sul depocenter, especially the deposits that follow the Lontras Shale (transition between Unit A and Unit B), which have high thickness. Notice the highest thickness of Lontras Shale, nearby Rio do Sul Locality (1MB01).

The maximum flooding surfaces demonstrated easier recognition on well logs and were used as a datum on the correlations. In turn, the stratigraphic architecture interpretation followed the sequence stratigraphic concepts proposed by Hunt and Tucker (1992) in which the sequence boundaries (SB) and their correlative conformities (CC) are supposed to represent the end of base-level fall.

The term rhythmite is referred to as thin-bedded, regular alternations of silt, clay, and very fine sand, while the term diamictite followed the classification of Flint *et al.* (1960) that describes diamictites as matrix-supported sedimentary rock, poorly sorted, resulting from the mixture of mud, sand, and gravel. Likewise, the terminology of Mulder and Alexander (2001) was applied for subaqueous sediment gravity-flow deposits, in which low-density flows (<9% of sediment concentration) are truly turbulent (e.g., Middleton and Hampton 1973) and define turbidity currents (*sensu stricto*); meanwhile, the terms concentrated and hyperconcentrated density flows (noncohesive density flows) indicate the presence of grain-to-grain interactions and turbulence together as support mechanisms.

STRATIGRAPHIC FRAMEWORK

The study interval in the Rio do Sul area embraces a sedimentary succession of up to 500-m thick, which comprises three depositional units: the basal unit (Unit A) with a fining-upward pattern that culminates with a mud-rich interval, an intermediate succession showing a coarsening-upward pattern (Unit B), and a new fining-upward succession (Unit C).

Unit B is divided into Unit B upper and lower. The whole interval is composed of 18 sedimentary facies whose descriptions and interpretations are presented in Table 1. We defined nine main facies associations that are recurrent in different depositional units:

- subglacial to ice-marginal deposits;
- deep-marine mudstones or offshore mudstones;
- thin- and thick-bedded turbidite deposits;
- hyperconcentrated and concentrated density-flow deposits (CDFD);
- mass transport deposits (MTD);
- prodeltaic deposits;
- delta-front and shoreface deposits;
- delta-plain deposits;
- fluvial-dominated, coastal plain deposits (Table 2 and Figs. 3-5).

Depositional units

Unit A: glacial and proglacial to deep-marine deposits

Up to 80-m thick, this unit is composed of three facies associations that exhibit a general fining-upward trend (Figs. 3, 4, and 6). The lower boundary characterizes the major nonconformity on Precambrian basement rocks with well-developed glacial striae. At the base, there is an association dominated by massive diamictites Dm(s) followed by resedimented diamictites Dm_(r). Instead, at some places, we can observe a facies association composed of conglomerates and conglomeratic sandstones. This succession is covered by rhythmites and

Table 1. Summary of sedimentary facies recognized and interpreted in the Rio do Sul depocenter, southern Brazil, Pennsylvanian-Permian, Paraná Basin.

Facies	Description	Interpretation
Gm	Massive to crudely stratified paraconglomerate, with clasts of granite, sandstone, gneiss, schist, and quartz, within sandy to muddy-sandy matrix; grain size varies from granules to cobbles, some of them striated and faceted.	Deposition of concentrated density flows (Mulder and Alexander 2001).
Sm _(g)	Fine to medium grained and massive sandstones, poorly sorted, with floating and extrabasinal granules to pebbles in muddy-sandy matrix. It can contain dish structures and large rip-up clasts at the base.	Deposition of hyperconcentrated to concentrated density flows (Mulder and Alexander 2001).
Sm _(f)	Very fine and massive sandstones, poorly sorted, with muddy-sandy matrix.	Deposition of turbulent flow (Bouma 1962, Mulder and Alexander 2001).
Sp/St	Trough/planar cross-stratified, medium to coarse sandstones, moderately to poorly sorted.	Migration of subaqueous dunes, bedload-dominated, hydrodynamic flows under lower flow regime (Miall 1978, 1996, 2006).
Sh/Sl	Fine to medium sandstone with low-angle cross-stratification (< 15°) or plane bedding, moderately to well sorted, with silt and very fine sandy matrix content.	Migration of subaqueous dunes, bedload-dominated, hydrodynamic flows under upper flow regime (Miall 1978, Tucker 2003).
Shc	Fine to medium sandstones, moderately to well sorted, with very fine and silt matrix content and hummocky cross-stratification.	Deposition of oscillatory flows, in which migration of symmetric subaqueous dunes develop concave-concave truncation (Tucker 2003).
Sd	Fine sandstones, moderately sorted, with soft-sediment deformation.	Penecontemporaneous deformation due to loading and fluid scape (Tucker 2003).
Sr/Sr _(w)	Very fine to medium sandstones, poorly to moderately sorted, with asymmetric (including climbing ripples) or symmetric ripples. The symmetric ripples contain muddy and organic drapes.	Migration of subaqueous current or wave ripples, under lower flow hydrodynamic regime (Miall 1978).
Shl	Very fine sandstones, moderately sorted, with planar lamination.	Deposition of traction bedload-dominated hydrodynamic process under lower flow hydrodynamic regime (Miall 1996).
Dm	Massive rocks with rounded to angular, polymictic granules to boulders dispersed in a muddy to sandy-muddy matrix (diamictites). In places, shear surfaces are present. Clast compositions include gneisses, schists, quartzite, siltstone, sandstones, TBT, and plant fragments.	Deposition of subaqueous mass movements characterized by complete homogenization of the mass flow (Eyles <i>et al.</i> 1983, Shanmugam 2006).
Dm _(f)	Massive rocks with rounded to angular polymictic granules to boulders dispersed in a muddy to sandy-muddy matrix (diamictites). Structures of penecontemporaneous deformation (faults, shear surfaces, and folds) are present. Clast compositions include gneisses, schists, quartzite, siltstone, and sandstones. Allochthonous deltaic and TBT blocks occur as rafted blocks.	Deposition of subaqueous mass movements (slides and slumps, Eyles <i>et al.</i> 1983, Shanmugam 2006).
Dm _(s)	Homogeneous and sandy diamictites comprising floating clasts and subhorizontal anastomosing shear planes (millimetric spaced) and striated surfaces at the top. The clasts (granules and pebbles) are faceted and with basement affinity (granite and quartz).	Debris deposition and homogenization by shear due to the advancing glacier configuring subglacial tillites (Evans <i>et al.</i> 2006).
Dm _(d)	Sandy diamictites, roughly stratified, with flat base and asymmetric concave top layers in multiple lateral arrangements with dispersed granules and pebbles (of compositional affinity with the basement).	Released sediments from iceberg building iceberg-dump structures; the depletion of the fines, by dispersion in water, would cause the partial particles sorting (Thomas and Connell 1985).
Fl/Fl _(d)	Thinly laminated mudstones with or without dispersed clasts (dropstones).	Mud settling is occasionally associated with the deposition of ice-rafted debris.
Hl	Discontinued alternation of mudstones and very fine sandstones, with current ripples, composing linsen heterolithic structures.	Deposition of mud settling predominated over migration of subaqueous ripples, under lower flow hydrodynamic regime (Tucker 2003).
Hw/Hw _(w)	Discontinued alternation of mudstones and very fine sandstones, with current and/or wave ripples, composing wavy heterolithic structures.	Deposition of similar rates of mud settling alternating with migration of subaqueous current and/or wave ripples, under lower flow hydrodynamic regime (Tucker 2003).
Hf/Hf _(w)	Discontinued alternation of mudstones and very fine sandstones, with current and/or wave ripples, composing flaser heterolithic structures.	The result from the migration of subaqueous current and/or wave ripples, under lower flow hydrodynamic regime, predominated over mud settling (Tucker 2003).
C	Thinly laminated coal layers (vitrinite).	Deposition on vegetated swamp (Miall 1978, 1996).

Source: adapted from Schemiko *et al.* (2019).

Table 2. Facies associations present in the Rio do Sul depocenter, southern Brazil, Pennsylvanian-Permian, Paraná Basin.

Facies	Facies association/environmental setting	Occurrence in Depositional Units
Dm _(d) , Dm _(s)	Subglacial to ice-marginal deposits	A and B
Fl/Fl _(d)	Deep-marine mudstones or offshore mudstones	A, B, and C
Sr, Shl, Sm _(f) , Fl	Thin and thick-turbidite deposits	A and B
Gm, Sr, Sh, Sl, St, Sm _(g)	Hyperconcentrated and concentrated density-flow deposits	A and B
Dm, Dm _(e)	Mass transport deposits	A and B
Fl, Hl	Prodeltaic deposits	B
St, Sp, Sh, Sl, Sr, Sr _(w) , Sd, Shc, Shl, Hw, Hw _(w) , Hf, Hf _(w)	Delta-front and shoreface deposits	B and C
Sp, Sl, St, Hl, Hl _(w) , Sr _(w) , Fl, C	Delta-plain deposits	B and C
St, Sp	Fluvial-dominated, coastal plain deposits	B and C

Source: adapted from Schemiko *et al.* (2019).

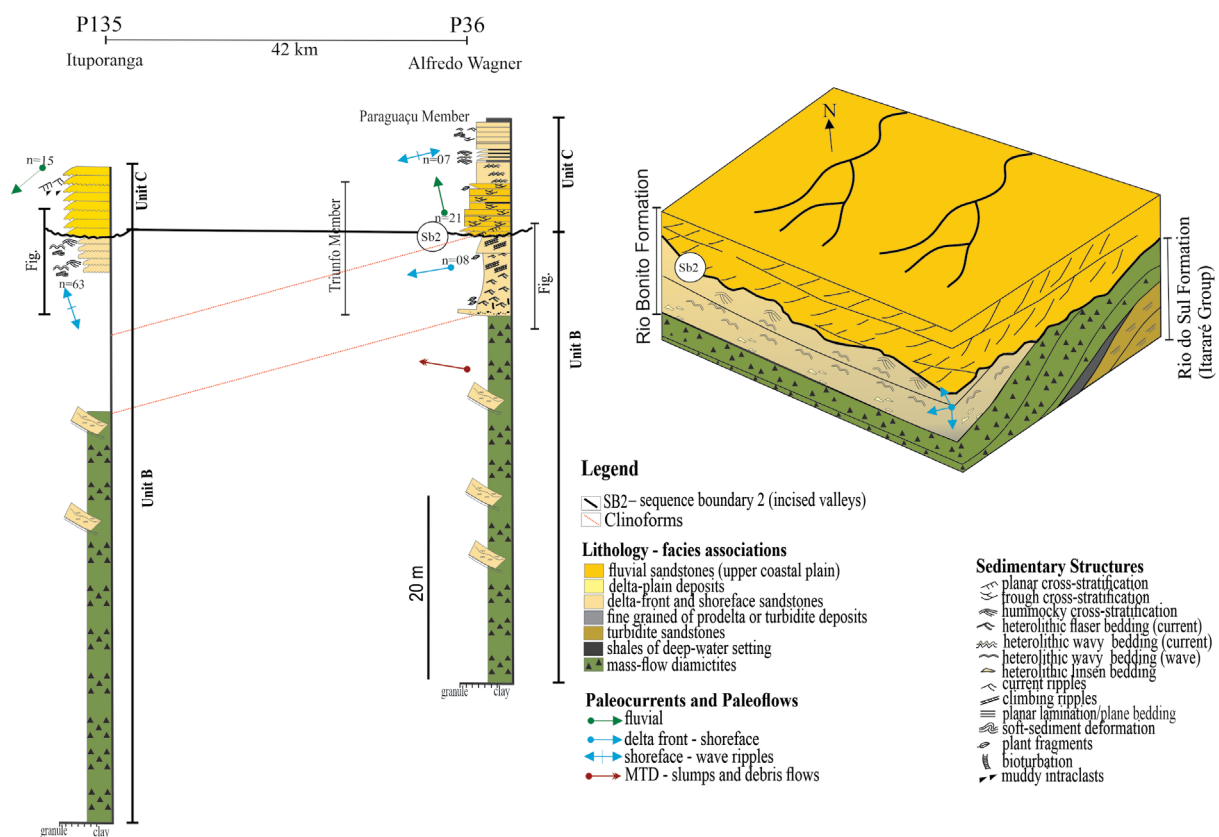


Figure 5. Problematic of the stratigraphic boundary between the Rio do Sul (Itararé Group) and Rio Bonito (Guatá Group) formations. The lithostratigraphic boundary can be established below SB02 (incised valleys), in the first deltaic sand bodies, or above SB02.

black shales, composing a package that can reach up to 50 m in thickness. These shales may show a south-southeastward onlap onto the basement rocks (Fig. 6F). In general, the unit is ascribed to the upper portions of the Mafra Formation and the lower strata of the Rio do Sul Formation. This succession corresponds to the depositional sequence S2 of Valdez Buso *et al.* (2019).

The basal Dm_(s) are poorly exposed and scarce throughout the study area and can be found, e.g., in the Presidente Getúlio region (Figs. 6A and 6B). Individual diamictite beds are irregular, about 0.5- to 2-m thick and laterally discontinuous. It sits directly on the Precambrian basement and is associated with

striated pavements. The facies Dm_(s) is composed of floating clasts within a sandy-muddy matrix (diamictites). The clasts are mainly in the granule and pebble fractions (< 5% of the rock volume), faceted, and with basement affinity (granite and quartz). This deposit has low-angle shear planes with millimetric spacing or foliation and striated surfaces at the top (Figs. 6A and 6B), allowing its classification as intraformational glacial surfaces (soft-sediment glacial surfaces; e.g., Visser 1990, Vesely *et al.* 2015, Rosa *et al.* 2016). It suggests, together with the clast characteristics, that Dm_(s) represents subglacial tillites (e.g., Evans *et al.* 2006) and likely lodgment tillites (Fallgatter and Paim 2017).

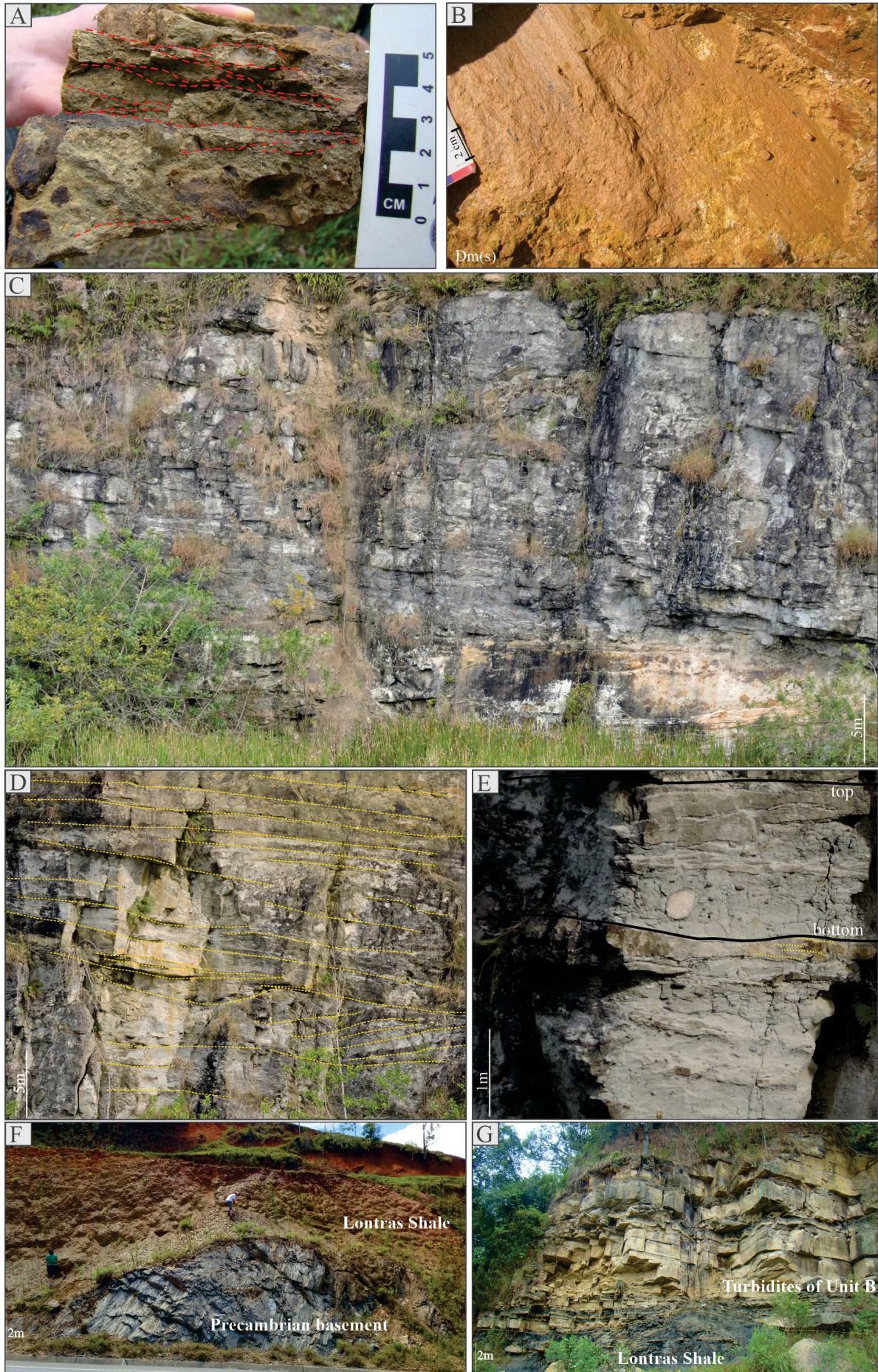


Figure 6. Main facies of Unit A and forms of occurrence of the Lontras Shale. Subglacial tillites with low-angle shear planes with (A) millimetric spacing or foliation and (B) striated surfaces at the top in the Presidente Getúlio locality. (C-E) Massive conglomerates and conglomeratic sandstones stratified into tabular and lenticular strata, configuring sets (yellow lines) of amalgamated beds, obliquely arranged (José Boiteux locality). (F) Contact between the Lontras Shale and Precambrian basement (Vidal Ramos locality). (G) Contact between the Lontras Shale and the turbidite beds of Unit B (Doutor Pedrinho locality).

The diamictites $Dm_{(r)}$ configure a package of about 5-m thick. It consists of a muddy-sandy matrix with dispersed out-sized clasts (up to 1 m) composed of sandstones and rhythmites and granule to boulder clasts derived from the basement rocks, some of them striated and faceted. They can be massive and show folded bedding planes, fractures, faults, and shear surfaces. The last structure usually bound outsized clasts with sedimentary affinity. Such features allow us to interpret them as MTD (cf. Shanmugam and Moiola 1988, Shanmugam 2006, Shanmugam and Wang, 2015). The basement-affinity clasts within the fine-grained matrix point to the resedimentation of ice-rafted debris (e.g., Fallgatter and Paim 2017, Mottin *et al.* 2018, Valdez Buso *et al.* 2019).

Above the basal tillites and mass flow diamictites, or in place of, there are coarse-grained deposits composed of polymictic conglomerates and conglomeratic sandstones. They can be massive or display diffuse stratifications and ripples with floating and extrabasinal granules to pebbles in a muddy-sandy matrix (facies Gm, Sr, Sh, Sl, St, and $Sm_{(g)}$). These clasts are often striated and faceted. The conglomeratic layers can be up to 50-m thick (José Boiteux locality), forming a set of lenticular and tabular beds, and obliquely arranged, with erosional and concave-up base. These strata are interpreted as deposition products of concentrated density flows derived from melting water discharge of retreating glaciers (Figs. 6C-6E), i.e., subaqueous outwash fans (Aquino *et al.* 2016). Valdez Buso *et al.* (2019) ascribed their erosive base to a sequence boundary due to the glaciotectonic features impressed over the previous deposits (Aquino *et al.* 2016). According to Aquino *et al.* (2016) and Fallgatter and Paim (2017), these deposits are also exposed around the Doutor Pedrinho (northern) and Alfredo Wagner (southern) localities and are associated with thick-turbidite deposits.

Rhythmites followed by black shales overlie the basal interval encompassing tillites, diamictites, and coarse-grained deposits (Figs. 6E-6G). The rhythmites consist of tabular-shaped siltstone alternated with black shale composing mm-scale couplets. It grades upward to a thick package composed of fissile black shale, which has occasional carbonate lenses with a cone-in-cone structure. Basement-affinity clasts (granule to a boulder) occur in the muddy layers. This facies association is understood as the result of mud fallout and deposition from dilute suspension plumes in a somewhat deepwater environment (Miall 1978, Eyles *et al.* 1983), while the basement-affinity clasts interpreted as dropstones point to the influence of floating ice. The origin of carbonate lenses is most likely an early diagenetic process and means an extremely low clastic sedimentation rate (Schemiko *et al.* 2019). The association corresponds to the Lontras Shale, which is a basin-scale stratigraphic marker (França and Potter 1988). It is interpreted herein as a maximum marine transgression developed subsequently to an ice-margin retreat (e.g., Valdez Buso *et al.* 2019).

Unit B: glacially influenced, co-genetic deep-marine to fluvio-deltaic deposits

Unit B has a general thickening/coarsening-upward trend and embraces nine facies associations, reaching up to 200 m in

thickness (Figs. 3 and 4). It starts with muddy- and sand-rich rhythmite over the Lontras Shales, followed by thick sandstones, conglomerates and conglomeratic sandstones, and diamictites, configuring the lower interval of Unit B (Fig. 7). An interval composed of heterolithic and sandstone-dominated deposits overlies the diamictites and sets up the Unit B upper (Figs. 5, 8, 9, and 10). Usually, the lowermost interval of this unit is assigned to the Rio do Sul Formation (Itararé Group, Schneider *et al.* 1974, Castro 1991). The Unit B upper, in turn, is referred to as Triunfo Member of Rio Bonito Formation (Guatá Group, Schneider *et al.* 1974, Castro 1991).

Unit B lower

The rhythmites (Figs. 7C and 7D) are characterized by thin and tabular layers of normally graded sandstone or siltstone layers (e.g., facies Sr, Shl, and $Sm_{(r)}$) rhythmically alternated with black mudstones with dispersed basement-derived clasts (granule to cobble, facies Fl, and $Fl_{(d)}$). These pass upward to thicker (> 50 cm) tabular or lenticular packages, with an erosive base (0.5–1 m, Figs. 6G and 7D), composed of normally graded sandstones comprising incomplete Bouma sequences. The thin and thicker sandstones show several sole marks, such as flutes, prods, bounce, and grooves. The rhythmite characteristics are consistent with the model of thin-bedded turbidites (TBT; cf., Mutti 1962), whereas the key features of the thick sandstones point to the deposition from surge-type turbidite currents (Bouma 1962, Lowe and Guy 2000, Mulder and Alexander 2001, Mulder *et al.* 2003). The dispersed clasts with basement affinity attest to the glacial influence during the deposition.

The following facies association comprises conglomerates and conglomeratic sandstones (Figs. 7E and 7F), composing oblique and amalgamated bedsets (up to 10-m thick and 30-m wide). It rests on concave-up erosive surfaces whose interface can show penecontemporaneous deformations (e.g., faults and folds). In some cases, massive sandstones contain erosive bases with large rip-up clasts (up to 30 cm) from underlying rhythmites. Each layer has a pattern of normal or inverse gradations. Conglomeratic sandstones or massive conglomerates pass upward to sandstones with diffuse stratifications or laminations. The inverse also may occur. Some pebble-to-boulder clasts are striated and faceted, and others occur aligned parallel to stratifications and laminations (Figs. 7E and 7F). These characteristics suggest the deposition from concentrated and hyperconcentrated density flows according to the classification of Mulder and Alexander (2001), in which vertical facies oscillations are attributed to hyperpycnal flows due to the fluctuating melting water discharge pointed out by striated and faceted clasts (hyperpycnites, Schemiko *et al.* 2019).

An up to 100-m-thick interval composed of diamictites covers or is laterally associated with the above-described noncohesive density-flow deposits (Figs. 7A and 7B). The diamictites are typically massive and composed of clasts immersed in a sandy-muddy matrix. The size range of the clasts embraces granules to boulders of igneous-metamorphic composition, which can be faceted and striated. However,

many diamictites have plant fragments and intrabasinal out-sized clasts (dimensions ranging from 0.5 to 10 m, Fig. 7B) of sandstones and rhythmites, usually bounded by shear surfaces $Dm_{(p)}$. Sandstone blocks show sedimentary structures observed in overlying facies associations such as heterolithic bedding, current and wave ripples, trough cross-stratification, and plant debris. These sedimentary structures become challenging to identify in the higher homogeneous facies (Dm) due to penecontemporaneous deformations such as folds and faults. Heterogeneous clasts dispersed in a sandy-muddy matrix can be interpreted as the deposition product of gravity flows with cohesive behavior. Thus, the blocks with recognizable sedimentary structures can be described as rafted blocks, while

the penecontemporaneous deformations attest to the plastic behavior. It supports the interpretation of MTD from slope failure for these deposits (cf. Shanmugam and Moiola 1988, Shanmugam 2006, Shanmugam and Wang 2015).

The structures related to shallow environments within the large rafted blocks point to the deposition origin associated with slides from the collapse of an unstable shelf edge or deltaic slope. In turn, the presence of plant debris inside blocks suggests a deglaciated shoreline during the failure. The occurrence of striated and faceted clasts indicates the contribution of ice rafting (Schemiko *et al.* 2019) and/or the remobilization of prodeltaic facies such as thin-bedded rhythmites with dropstones (Rodrigues *et al.* 2021).

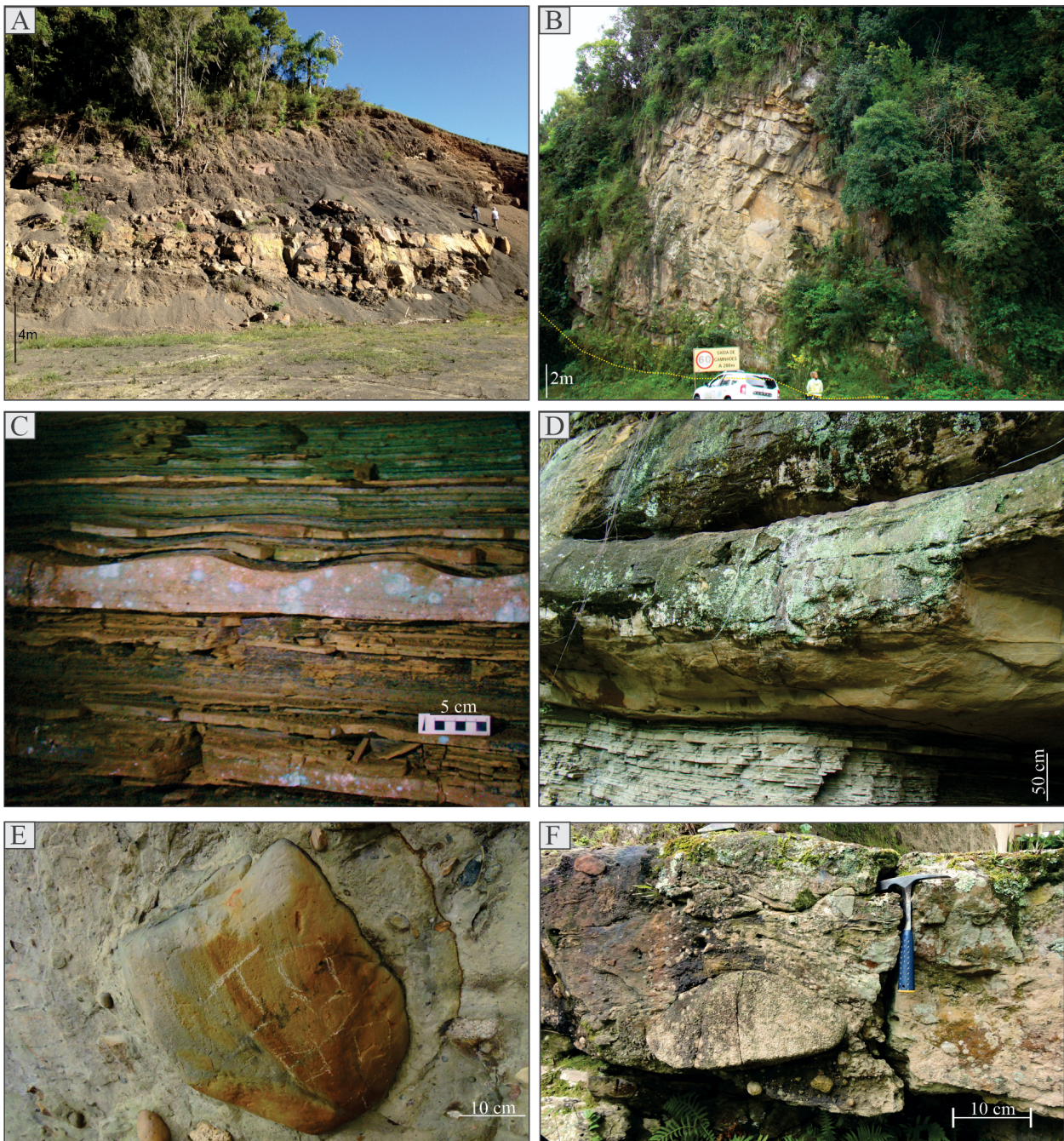


Figure 7. Main gravitational flow deposits of Unit B. (A) Sandstone boulders within mass transport deposits (MTD, Alfredo Wagner locality). (B) Delta sandstone boulders immersed in a sandy-muddy matrix of the MTD (Alfredo Wagner locality). (C) Thin-bedded turbidites with current ripples (Vidal Ramos locality). (D) Contact between thin- and thick-bedded turbidites (Vidal Ramos locality). (E and F) Faceted and striated clasts within the concentrated density-flow deposits (Presidente Getúlio locality).

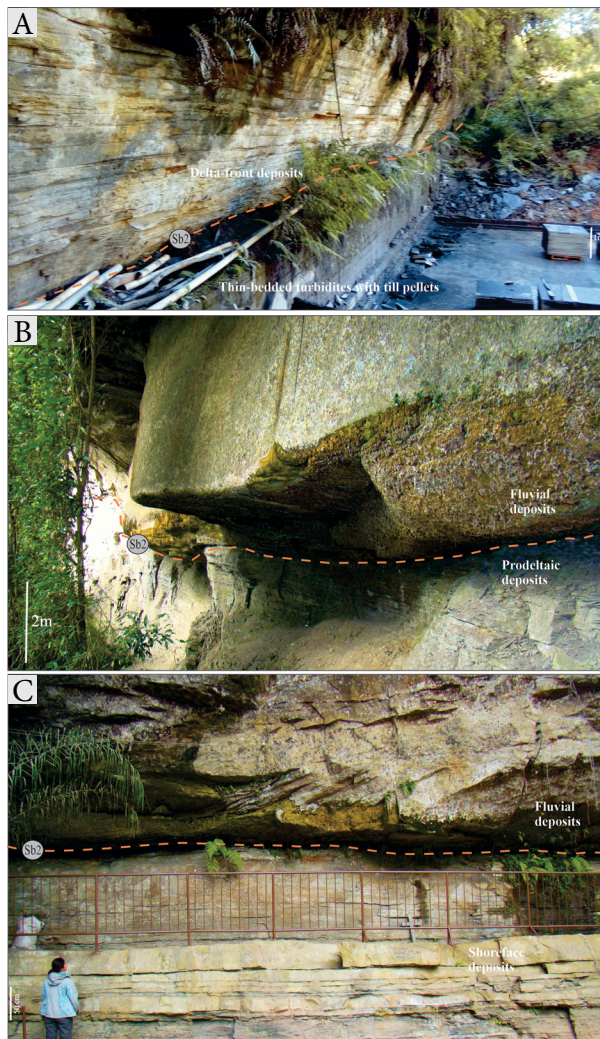


Figure 8. Contact relationships between upper Unit B and the basal fluvio-deltaic strata of Unit C. (A) The contact between thin-bedded turbidites bearing till pellets with delta-front deposits in the Trombudo Central locality. (B and C) Subaerial unconformity SB2 over the prodeltaic (P14 in Rio do Oeste locality) and shoreface (P135 in Ituporanga locality) deposits.

Unit B upper

The Unit B upper overlies the MTD and/or noncohesive density-flow deposits and composes coarsening and thickening-upward parasequences (Figs. 3-5). At the base, there are laminated mudstones (Fl) overlain by linsen-bedded heterolithic deposits (Hl, Figs. 8C and 9E). Upwards, the succession becomes coarse grained, showing way to flaser heterolithic packages (H_w , $H_{w(w)}$, H_f , $H_{f(w)}$), followed by laminated and stratified sandstones in tabular beds at the top (Figs. 8B, 8C and 9A-9D). The heterolithic packages may appear amalgamated with sandstone bodies. These sandstones display hummocky (Shc), trough and low-angle cross-stratification (St and Sl), as well as plane bedding (Sh), convoluted folds (Sd), and wave and current ripples (Sr and $Sr_{(w)}$), with or without muddy- and organic-rich drapes. In this context, bioturbations are common, such as Skolithos. Clasts with basement affinity are present in the muddy facies but are scarce (e.g., P71, Presidente Getúlio locality). The basal, muddy facies may be

interpreted as prodeltaic deposits, and the uppermost sandier facies are ascribed to the delta-front and shoreface deposits (Schemiko *et al.* 2019). The occasional clasts with basement affinity are understood as dropstones and point to some glacial influence (e.g., Castro 1991).

Towards the top, the delta-front and shoreface deposits are replaced by a facies association characterized by the presence of poorly sorted sandstones with trough and planar cross-stratification, bioturbations (Skolithos), and paleosols with Bk horizon (Schoeneberger *et al.* 2012). The sandstones are interbedded with thin and lenticular heterolithic packages associated with coal layers (C). In this context, plant fragments and pyrite concretions are also frequent. Particularly, the sandstones are feldspathic and medium to coarse grained, comprising amalgamated and nonamalgamated beds (0.3–1-m thick) with an erosive and concave base forming cut-and-fill structures. These features suggest deposition on the delta-plain environment (Bhattacharya 2006, 2010, Rossi and Steel 2016).

In addition, in the Trombudo Central region, nearby Rio do Sul area, and in the same stratigraphic level of the shallow-marine deposits (e.g., shoreface), there are thinly laminated sandstones with sinusoidal current ripples and till pellets rhythmically alternated with black mudstones or siltstones with dropstones, some of them oversized (Fig. 10). It contains raindrop craters and jumping trackway assigned to arthropods (Silva *et al.* 2021) and microbial mats (Noll and Netto 2018). These rhythmites may be interpreted as TBT (e.g., Santos *et al.* 1992, Tedesco *et al.* 2020) due to the freshwater input from glaciers melting into the supratidal environment (Lima *et al.* 2015, Noll and Netto 2018) with fluctuating water levels and consequently temporary exposure of the substrate (Silva *et al.* 2021). The turbidites are interbedded with beds of a flat base and asymmetric concave top (> 50 cm wide and < 50 cm thick) disposed in multiple lateral arrangements (Fig. 10A). It is composed of roughly stratified material of sandy-muddy composition with dispersed granules and pebbles (of compositional affinity with the basement). We interpret these beds as deposition-related structures from iceberg-released sediments named iceberg-dump structure (Thomas and Connell 1985). Soft-sediment glacial surfaces occur between the layers of the TBT (Figs. 10B and 10C), which were previously reported and interpreted as iceberg scour marks resulting from scouring of floating ice on subaqueous sediments (Santos *et al.* 1992).

Unit C: postglacial, fluvio-deltaic to deep-marine deposits

Unit C is up to 50-m thick and rests on Unit B by means of an erosive surface (Figs. 3-5, 8, and 9F). This unit is like the uppermost shallow-marine deposits of the previous one; however, it shows a fining-upward stacking pattern. Thus, the upper Unit B is covered by strata composed of poorly sorted and stratified sandstones (St, Sl, and Sp) with muddy intraclasts and a concave-up base. It configures amalgamated bedsets that can reach thicknesses greater than 6 m and is understood as fluvial deposits, usually ascribed to the Triunfo Member of the Rio Bonito Formation (Zacharias and Assine 2005).

These fluvial deposits cut down mainly the delta-plain (Presidente Getúlio locality, Fig. 3) and shoreface deposits (Ituporanga locality, Fig. 8C), or even it can erode prodeltaic deposits (Rio do Oeste locality, Fig. 8B), MTD (Figs. 3 and 4), and proglacial deposits (Trombudo Central locality, Fig. 8A). Therefore, we interpret this erosive surface as a subaerial unconformity that is recognized throughout the study area, configuring an incised valley (e.g., Zacharias and Assine 2005, Schemiko *et al.* 2019). After fluvial expression, tidal-influenced delta deposits (and/or estuarine deposits — Zacharias and Assine 2005, Tognoli 2006) and mud-rich strata fill the incised valley, as observed in the Alfredo Wagner

region (P36, Fig. 5). The mud-rich interval is assumed here as distal offshore deposits of Paraguaçu Member (Rio Bonito Formation, e.g., Tognoli 2006).

Stratigraphic correlation

The stratigraphic stacking patterns recognized in outcrops for the study interval at Rio do Sul region were also detected in wells (Petrobras and CPRM) throughout hundreds of kilometers into the basin (Figs. 3 and 4).

The proglacial to deep-marine deposits of Unit A are correlated to a basal interval with fining-upward pattern, in which the coarse-grained facies have low radioactivity at the base of

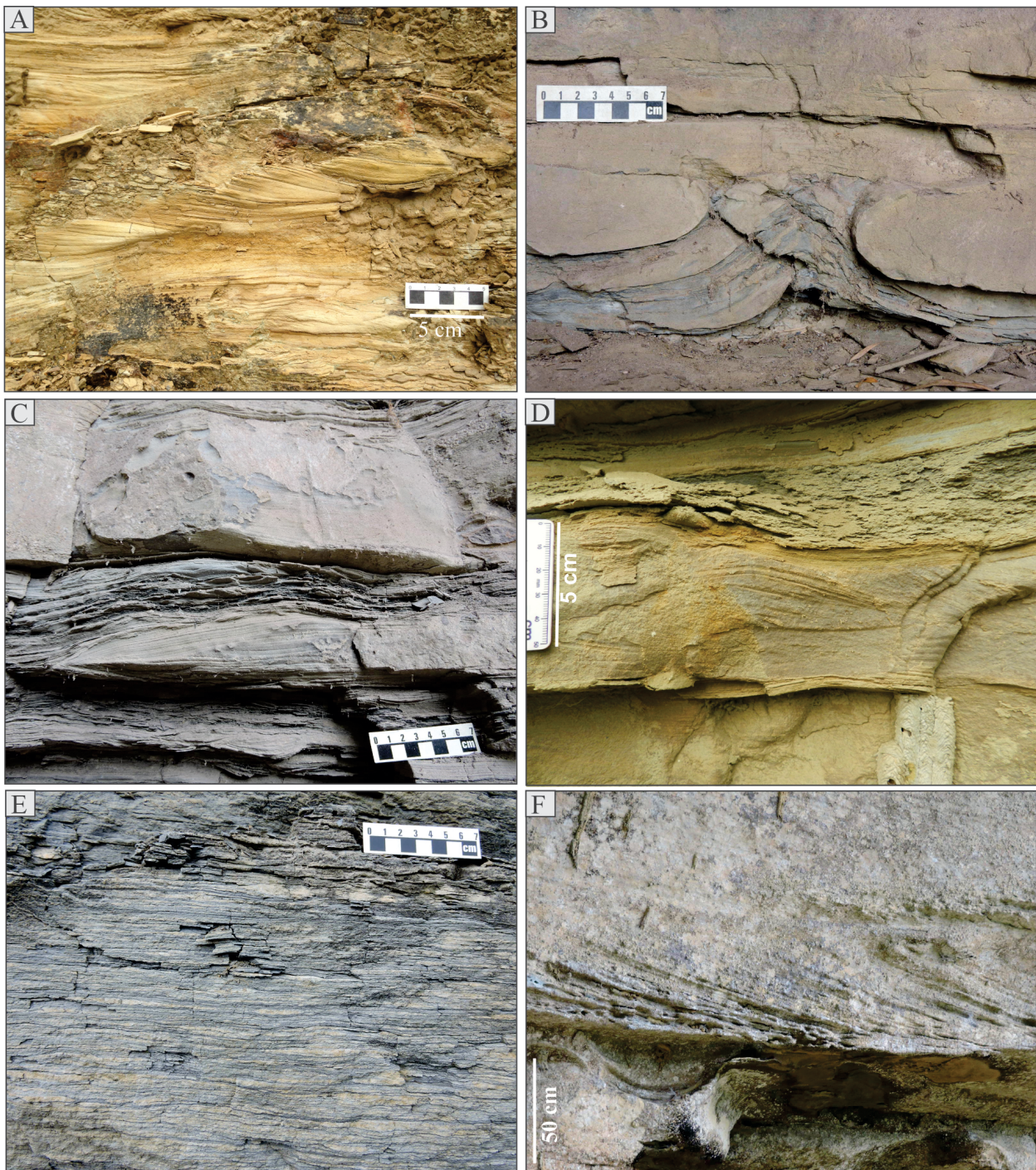


Figure 9. Main fluvial and fluvio-deltaic facies of Unit B and Unit C. (A) Current ripples of delta-front deposits of Unit B. (B) Convoluted folds in silty sandstones in a delta-front context (Unit B). (C and D) Hummocky cross-stratification in shoreface deposits of Unit B. (E) Flaser heterolithic deposits of prodelta (Unit B). (F) Planar cross-stratification in fluvial strata of Unit C above the subaerial unconformity SB2.

the unit, showing bell or cylindrical shape. The succession progressively becomes an interval with an irregular (saw tooth) shape pattern at the top, which has relatively higher gamma-ray counts and correlates to the topmost rhythmites of Unit A.

The contact between Units A and B is characterized by the peak of high radioactivity at the top of the lowermost

unit that defines the correlation datum, corresponding to the Lontras Shale. The peak is followed by succession with a coarsening-upward pattern that characterizes the Unit B stacking. This pattern is well marked in outcrops and well logs. Usually, the peak of high radioactivity is followed by boxcar and/or cleaning-up trend (irregular or funnel shape) related to the

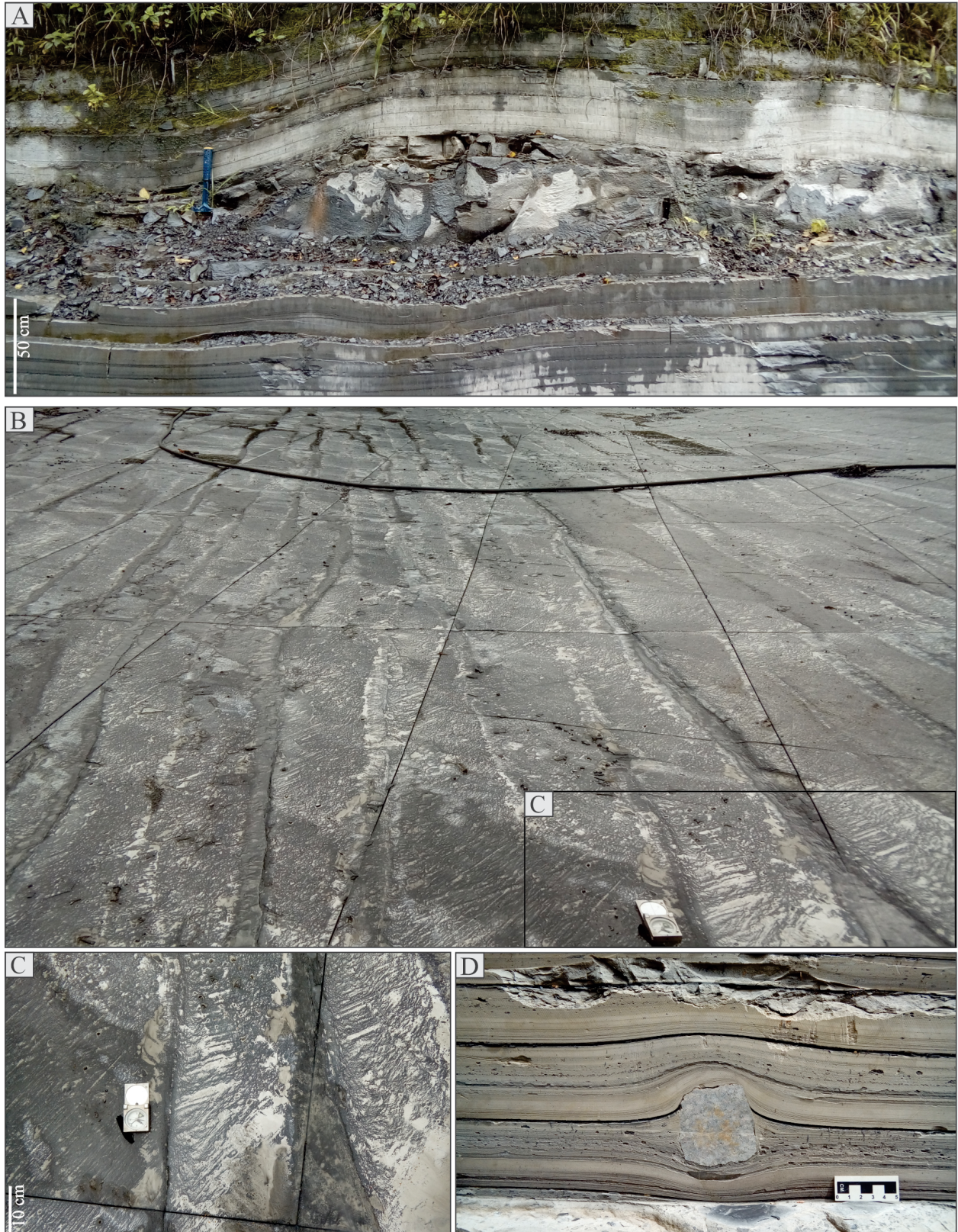


Figure 10. (A) Dump structures interbedded with thin turbidites with till pellets present in Trombudo Central locality, nearby Rio do Sul locality. (B and C) Possible intraformational glacial surfaces (soft-sediment glacial surfaces) with WSW-ENE direction. (D) Details of thin-bedded turbidites with till pellets, in which dropstones of quartz composition can also be observed.

TBT and thick-bedded turbidites or hyperconcentrated density-flow deposit and CDFD. It grades upward (or is laterally disposed of) to the irregular shape corresponding to the diamictites. The diamictites, in turn, are followed by a cleaning-up trend (funnel shape) related to the deltaic progradation. Based on outcrop data, the diamictites hold rafted blocks composed of deltaic facies, showing a clear genetic relationship with the upper deltaic facies (shelf-margin delta, Schemiko *et al.* 2019). Thus, the low radioactivity peaks within the irregular shape may represent deltaic sandstones by means of interbeds or allochthonous blocks.

The mud-rich interval corresponding to the Lontras Shale (Rio do Sul Formation) is a commonly used regional datum (Vesely and Assine 2006) understood here as the last level of black shale with the highest radioactive peak before the uppermost deltaic progradation frequently referenced as Rio Bonito Formation. In this way, the Passinho Shale (Santos *et al.* 1996) documented above the Lontras Shale (Daemon and Quadros 1970, Rocha-Campos and Rössler 1978, Santos *et al.* 1996, Vesely 2006) is here assigned to the prodeltaic muddy strata of the Rio Bonito Formation (e.g., Popp 1983, Castro 1991; Fig. 3). Stratigraphic correlations recorded in the literature show these shales superimposed by the sandstone-rich deltaic deposits of the Rio Bonito Formation (Vesely 2006) or laterally disposed to the deltaic sandstones (Rocha-Campos and Rössler 1978). According to this approach, the Lontras Shale does not necessarily correspond to the range of shales slightly above the Precambrian basement as proposed by Fallgatter and Paim (2017), although it is often arranged in this way (Fig. 6F).

The inversion of the stacking pattern characterizes the passage from Unit B to Unit C, highlighting the subaerial unconformity from which starts a retrogradational stacking pattern that delineates Unit C. At the base of this interval, the low radioactivity peaks represent fluvial sandstones with cylindrical or funnel shapes. It grades upward to relatively higher gamma-ray counts, corresponding to estuary deposits that culminate with the siltstones and shales correlated with the Paraguaçu Member (e.g., Tognoli 2006). In this context, nearby Rio do Sul area, there is the preservation of delta-plain deposits under subaerial unconformity (Fig. 3), while on other localities the basal fluvial deposits of Unit C occur directly over the MTD, prodelta or shoreface deposits of Unit B (Figs. 3-5 and 8).

Sediment transport and fill patterns

Paleocurrent patterns for Unit A were not recorded in this study once previous works have documented it satisfactorily. A detailed study of the basal nonconformity carried out by Fallgatter and Paim (2017) shows partially exhumed glacial troughs and gouges into the Precambrian basement associated with lodgment tillites. These features have a consistent NW orientation. According to Aquino *et al.* (2016) and Fallgatter and Paim (2017), the conglomeratic facies association (subaqueous outwash fans) is also exposed around Pedrinho and Alfredo Wagner, respectively, and shows paleocurrents mainly toward NW, where

NE and SW are secondary components (Fig. 3). Likewise, Rodrigues *et al.* (2021) point to general paleoflows toward the N for uppermost folded rhythmites (classified as incipient MTDs) at Presidente Getúlio locality.

About 700 paleocurrent measurements were obtained from cross-stratifications and current ripples in sandstones and sandy rhythmites of Unit B. In general, these data refer to TBD and thick-bedded turbidites, hyperconcentrated density-flow deposit and CDFD (hyperpycnites), shoreface, and delta-plain deposits. Based on the trends of the sediment transport in this depositional unit, the studied area can be subdivided into three major sectors (regions):

- Presidente Getúlio-Witmarsum (north-northeastern), where paleocurrents are to the south-southwest;
- Rio do Sul (center-eastern) with paleocurrents toward the west;
- Vidal Ramos-Alfredo Wagner (southern), showing paleocurrents mainly to the northwest and, secondarily to the southwest (Figs. 2 and 3).

Conglomeratic facies of noncohesive density-flow deposits are present mainly in the Presidente Getúlio (northern sector) locality and are genetically associated with uppermost thick turbidites showing paleocurrents toward the south-southwest (Schemiko *et al.* 2019). In this locality, the paleocurrents of TBT are chiefly toward the northwest, which is the same orientation obtained from thick-bedded turbidites and TBT present in the localities of Vidal Ramos and Alfredo Wagner (southern sector), where the conglomeratic facies are absent. Consequently, the TBT seem to be genetically related to a slope-parallel paleoflow direction sourced from areas farther to the SE.

In the Witmarsum locality (northern sector), the kinematic analysis of the MTD carried out by Rodrigues *et al.* (2021) points to paleoflows toward the NW for more evolved mass flow diamictites (Figs. 2 and 3). In the south-southeast portion of the study area, in the Alfredo Wagner locality, the paleoflow pattern ranges from WNW to SW (Fig. 3), according to Rodrigues *et al.* (2021). Additionally, these data agree with the flow directions obtained through anisotropy of magnetic susceptibility (AMS) by Amato (2017) for these deposits in the regions of Aurora (NNW), nearby Vidal Ramos locality, and Alfredo Wagner (NW and W).

In the center-eastern, the soft-sediment glacial surfaces (iceberg scour marks) that occur in the stratigraphic level of shallow-marine deposits of Unit B have a WSW-ENE direction (Fig. 10), a similar direction obtained by Santos *et al.* (1992) for these features (WNW) at the same locality (Trombudo Central). In this context, the TBT with till pellets present paleocurrents to the WSW (Fig. 2).

Overall, the fluvial packages of Unit C, displayed above the subaerial unconformity, have paleocurrents (about 100 readings) toward the SW and, less common, northwest directions (Figs. 2, 3, and 5). On the contrary, subsequent delta deposits have southwestern paleocurrent directions (e.g., P36), but with a northeast component that can be attributed to the tidal process (drapes, Fig. 5, e.g., Mottin *et al.* 2018).

DEPOSITIONAL HISTORY

The deposition of study interval occurred in paleoenvironments ranging from shallow to relatively deep-marine deposits under different levels of glacial influence or with a lack of such influence. Glacial contribution during the sedimentation is evidenced by dropstones in distinct stratigraphic levels (Units A and B), striated and faceted clasts within mass flow diamictites and noncohesive density-flow deposits, and structures associated with floating ice, such as till pellets. Features that point to the tide activity evidence the marine environment (Units B and C). Marine setting is also supported by the presence of marine fossils like conodonts (Rocha-Campos and Rössler 1978, Simões *et al.* 2012, Wilner *et al.* 2012, 2016, Scomazzon *et al.* 2013, Neves *et al.* 2014) in the Lontras Shale (Unit A).

Through the recognition of depositional trends of each unit associated with the sediment transport pattern and spatial distribution, it is possible to reconstruct the depositional history of the study area. Therefore, three evolutionary stages are defined in this study. Yet, the depositional trends of each unit were recognized and traced up to 400 km into the basin. It points to the regional expression of these events, supporting the interpretation of the stratigraphic architecture and depositional evolution of the Rio do Sul depocenter (Figs. 3 and 4).

The first stage has the subglacial tillites and CDFD (Aquino *et al.* 2016, Fallgatter and Paim 2017, Valdez Buso *et al.* 2019) of Unit A as the expression of the maximum glacial advance over the Precambrian basement or on irregular surface scoured into the previous deposits (Valdez Buso *et al.* 2019), respectively, configuring a sequence stratigraphy boundary named as SB1

(Figs. 3, 4, and 11A). Mass flow diamictites and rhythmites superimposing these basal deposits point to deglacial process, whereas the following glacially influenced deepwater shales (Lontras Shale) record the marine maximum flooding (MFS1). In this scenario, the mean paleocurrents of the CDFD toward the NW (Aquino *et al.* 2016, Fallgatter and Paim 2017) coincide with the mean vector to the north of the striated surfaces on the lowermost unconformity described in Santa Catarina State (Rocha-Campos *et al.* 1988, Fallgatter and Paim 2017) as elsewhere in the Itararé Group (Vesely and Assine 2002, 2006, Vesely *et al.* 2015, Rosa *et al.* 2016).

In turn, the second stage, referring to Unit B, is characterized by a change in the stacking pattern and paleoflows (Figs. 11B-11E). The Lontras Shale is covered by a coarsening-upward succession that starts with deglacial (proglacial) deepwater deposits and includes thin and thick turbidites, hyperconcentrated density-flow deposit, and/or CDFD. It is followed by MTD and fluvio-deltaic deposits, showing a progradational pattern. In this setting, the genetic relationship between the uppermost shelf-margin deposits (Schemiko *et al.* 2019) and mass flow diamictites is evidenced by shallow-water sedimentary structures present within the allochthonous blocks of the MTD, such as wave ripples. In this way, the mass flow diamictites represent the remobilization of delta-front deposits to the relatively deepwater environment (e.g., D'Ávila 2009, Suss *et al.* 2014, Valdez Buso *et al.* 2019). Based on this, we support the hypothesis of the conformable transition between the Rio do Sul Formation and the lowermost Rio Bonito Formation (Triunfo Member). At the top, incised fluvial valleys bound

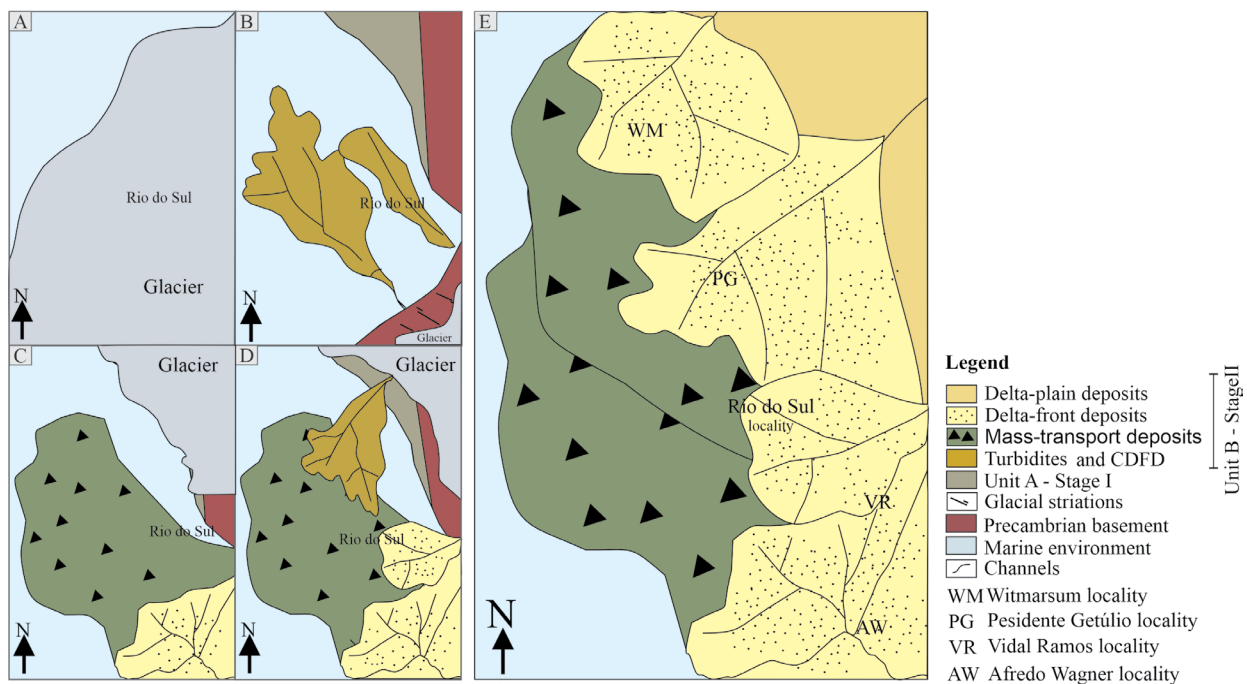


Figure 11. Evolutionary history and interpreted paleogeographic models for the Depocenter Rio do Sul, Pennsylvanian-Permian of the Paraná Basin, southern Brazil, with emphasis on the transition between Stage I and Stage II, which is time-equivalent of Cycle III of the Late Paleozoic Ice Age (LPIA). Glacial advance from SE (A) during the early Stage I that culminates with deposition of Lontras Shale. Sedimentation of turbidites after the development of Lontras Shale (B) toward NW. After, mass transport deposits (MTD) and genetically related fluvio-deltaic deposits were developed, with (C) NW and (D) W paleocurrents. (C) A new ice source is suggested from NE, based on striated and faceted clasts within concentrated density-flow deposits, (D) with paleocurrents to SW. (E) These deposits are genetically related to the MTD and the overlain fluvio-deltaic deposits, with the same sediment transport direction, configuring centripetal filling to the Rio do Sul depocenter over time.

this succession, configuring the second sequence stratigraphy boundary (SB2, Figs. 3-5 and 8).

Regarding the initiation of the mass transport, we argue that meltwater discharge was the trigger mechanism for slope instability due to the rapid input of sediments. It does not exclude that the faceted and striated clasts would have ice-rafted debris as a primary source during the early stages of deglaciation prior to incorporation into mass flow diamictites (e.g., Mottin and Vesely 2017). At the same time, those major floods may also be related to the development of concentrated and hyperconcentrated density flows by means of meltwater discharge bypassing the shelf to the deepwater (e.g., Mutti *et al.* 1996, Hubbard *et al.* 2010, Zavala *et al.* 2011), leading to the slope instability and sedimentation of the uppermost MTD. In this context, the quasi-steady density flows deposited those noncohesive density-flow deposits implying in relatively constant discharge for long periods (Kneller and Branney 1995, Mulder and Alexander 2001). Thus, the sediment supply possibly was from semi-continuous flood events produced by glaciofluvial discharge to deep-marine setting (Schemiko *et al.* 2019) instead of grounding-line fan systems as recorded elsewhere in the Itararé Group (e.g., Aquino *et al.* 2016, Fallgatter and Paim 2017).

The genetic relationship between deglacial deepwater deposits and fluvio-deltaic strata within Unit B is also evidenced by paleocurrent and paleoflow patterns. All facies associations have the same sediment transport showing a trend toward the northwest in the southern sector (Vidal Ramos-Alfredo Wagner region), west-northwest in the central sector (Rio do Sul — Trombudo Central region), and south-southwest in the northern sector (Vitor Meireles-Presidente Getúlio region). However, within this unit, we can still suggest some diachronism between the depositions of the center-southeastern and northern sectors. A progradational succession with south-southwest paleoflows in the northern sector seems to be developed over the basal TBT with NW paleocurrent genetic related to a primary progradational succession formed at central and southern regions (Schemiko *et al.* 2019). In those places, the stratigraphic relationship with the lowermost fluvial beds of Unit C indicates a transition between normal and forced regression, since the platform deposits as delta-front and shoreface beds occur under the fluvial-incised valley (SB2, Figs. 3-5 and 8). Likewise, fluvial beds (Unit C) rest on erosive and sharp-base contact with prodeltaic deposits (Rio do Oeste and Trombudo Central localities) and MTD (e.g., 1AL well, Fig. 4).

On the contrary, the second depositional succession from the north points to progradational-aggradational stacking pattern of co-genetic facies associations within clinofolds that offlap on the fluvial subaerial unconformity SB2 (Schemiko *et al.* 2019, Fig. 3), once the preservation of delta-plain deposits with tide influence evidence the normal regression conditions (highstand system tract, Catuneanu 2006). Consequently, the emplacement of MTD took place during the sea-level rise (Schemiko *et al.* 2019, Fig. 3). It is opposite to the classical sequence stratigraphic models (cf. Catuneanu 2006), in which thicker MTD are related to forced regression. Incised valley down-cutting interglacial highstand deposits were also

documented by Blum and Price (1998) for Texas Gulf Coastal Plain (Pleistocene Beaumont Formation).

The third stage that corresponds to the retrogradational stacking pattern developed over the SB2 began with fluvio-deltaic beds (Triunfo Member) deposition, followed by fine-grained deposits concerning the Paraguaçu Member (Fig. 5). The depositional trend suggests a transition from normal regression (lowstand) to transgression characterized by early infills of the incised valleys composed of tidal-influenced fluvial deposits (coastal plain, e.g., Rossi and Steel 2016) followed by estuary channels, composing the valley fill backstepping (Paraguaçu Member, e.g., Zacharias and Assine 2005). No feature related to glacial influence was observed in this stage.

According to the previous sequence analysis (Holz *et al.* 2006, 2010, Valdez Buso *et al.* 2019), the stacking pattern of each unit may be part of the two third-order depositional sequence in the Santa Catarina State (Fig. 1). Like Canuto *et al.* (2001), Valdez Buso *et al.* (2019) distinguished five deglacial cycles in the upper Itararé Group. Unit A corresponds to the depositional sequence 2 (Glacial Subcycle S2) of Valdez Buso *et al.* (2019), where the Lontras Shale expresses the marine maximum flooding from a deglacial process. After Lontras Shale deposition, the authors recognized additional three Glacial Subcycles (S3, S4, and S5). However, our findings suggest a genetic relationship between the glacially influenced deepwater deposits, developed slightly above Lontras Shales, and the upper shallow-water deposits under the incised valley. Thus, even assuming further Glacial Subcycles above the Lontras Shale at Rio do Sul depocenter, as proposed by Valdez Buso *et al.* (2019), we can still point to the genetic relationship between the last deglacial deposits (Itararé Group) and the superposed fluvio-deltaic deposits, usually assigned to Rio Bonito Formation.

PALEOGEOGRAPHY

The LPIA glaciation comprised major events (or cycles) also recognized across the Paraná Basin (Fielding *et al.* 2008, Valdez Buso *et al.* 2019). In this context, the evolutionary Stage I is time-equivalent to the upper Cycle II, whereas Stage II is related to Cycle III of the LPIA, the last major glacial event in the southern Gondwana supercontinent (Isbell *et al.* 2003, López-Gamundí and Buatois 2010, Valdez Buso *et al.* 2019). Paleogeography of multiple glacial lobes flowing into the Paraná Basin has been supported by several sedimentary features such as paleo-ice flow directions from subglacial landforms and soft-sediment grooving (Gesicki *et al.* 2002, Rosa *et al.* 2016, 2019, Fallgatter and Paim 2017) and paleocurrent patterns from deglacial deposits (e.g., Vesely *et al.* 2015, Aquino *et al.* 2016, Carvalho and Vesely 2017, Fallgatter and Paim 2017, Mottin *et al.* 2018, Mottin and Vesely 2021).

Similarly, there is a growth in studies supporting an NE-glacial source associated with the upper Itararé sedimentation (Mottin *et al.* 2018, Schemiko *et al.* 2019, Mottin and Vesely 2021). In this context, the results from this study would point to a change in the main paleo-ice flow direction between the upper Cycle II and Cycle III of the LPIA in the

Paraná Basin. Striations related to SB1 with NW direction and associated deglacial CDFD flowing toward NW (Figs. 3 and 6; Aquino *et al.* 2016, Fallgatter and Paim 2017, Valdez Buso *et al.* 2019) of Unit A indicate a sediment entry and glacial source area located at SE during the upper Cycle II (Stage I). However, faceted and striated clasts immersed in hyperpycnal density flows within Unit B in the north sector with paleoflows to the southwest also evidence an ice source to the NE at the end of the LPIA — Cycle III (Stage II; Figs. 2, 3, and 7).

Still, the study area comprises a particular paleogeography setting during the development of Stage II (Figs. 11B-11E). The transport pattern of co-genetic facies associations with the glacial influence of Unit B displays centripetal sediment feeding and glacial sources. In addition to the NE source, there are pieces of evidence of glacial sources to the E and SE. The upper Unit B in Trombudo Central locality (central sector) encompasses features pointing to the glacial source to the east-northeast and an extensive advance of ice to the W, such as TBT comprising till pellets and dropstones with paleocurrents to the west and southwest, as well as iceberg-dump structure associated iceberg scour marks with main ice flow direction toward the west (e.g., Santos *et al.* 1992; Figs. 2 and 10). In the south sector, the SE-glacial source is corroborated by TBT with dropstones and MTD with glacially derived faceted/striated clasts showing paleoflows to the NW (Figs. 2 and 7).

A northern source for diamictites with glacially derived faceted/striated clast of the Rio do Sul Formation is also present in the basin-scale lithofacies distribution as reported by França and Potter (1988) and Eyles *et al.* (1993), based on subsurface data. In the central-northern sector of the Paraná Basin, this diamictite-bearing unit is up to 200-m thick, extending horizontally over 700,000 km² (Eyles *et al.* 1993). According to França and Potter (1988), the passage toward the south of diamictite to dropstone-bearing shales and rhythmites points to the presence of a depocenter in the Santa Catarina State, configuring a proximal to distal architecture. Our results based on regional stratigraphic correlations and transport pattern also report the catchment area located to the NE but a further sediment feeding from E and NE for the diamictites, which pass to fine-grained deposits with glacial influence toward a main center nearby Rio do Sul locality (Figs. 3 and 4). This fill pattern is kept in the fluvio-deltaic deposition of Unit C (Triunfo Member). It would corroborate the hypothesis of a subsiding area in the south of the Paraná Basin, configuring the so-called “Rio do Sul” sub-basin (Canuto 1993).

Previous studies discussed the rate influence of tectonic and sea-level changes on the bounding relationships of the upper Itararé Group and lower Rio Bonito Formation. Tectonic uplift of the northeastern basin has been suggested based on fluvial paleocurrents to the SW of Rio Bonito Formation (Castro 1991, Milani and Ramos 1998, Milani 2004, Holz *et al.* 2006, 2010, Mottin *et al.* 2018). Therefore, in all hierarchical levels discussed here, regional and local, as well as based on both outcrop and subsurface data, it appears to be a tectonic overprinting on the eustatic signature creating space particularly recorded in the Rio do Sul depocenter, justifying the thickness and the transitional contact between those units. Thus, the

possible tectonic uplift began even during Itararé Group sedimentation, after Lontras Shales deposition, as can be observed by stratigraphic architecture and fill pattern of Unit B, not just after warm conditions of uppermost Rio Bonito Formation, as proposed by Holz *et al.* (2006).

Tectonic and deglacial processes may have provided a high rate of sediment influx. According to Porebski and Steel (2006), deltas are likely to form shelf-wide sand bodies within highstand systems tract mainly for fourth-order sequences (e.g., highstand shelf-margin deltas), on narrow and high-gradient shelves related to extremely high-discharge rivers from glaciated terrains or rising mountain belts. The late Quaternary Ganges-Brahmaputra delta is an excellent example of delta progradation, derived from high and sustained sediment supply combined result of tectonically active catchment and postglacial conditions, despite significant sea-level rise (e.g., Goodbred Jr. and Kuehl 2000, Goodbred Jr. *et al.* 2003), similar to the deltaic progradation-aggradation recorded in the north sector (Schemiko *et al.* 2019).

Also, the ages of the study interval are still an open matter for debate. The stratigraphic level regarding the genetic relationship between the shallow deposits of the lower Rio Bonito Formation and deep-marine deposits of the upper Rio do Sul (Taciba) Formation under SB2 is correspondent to Cycle S5 of Valdez Buso *et al.* (2019). According to recent dating, this interval is late Moscovian-early Kasimovian (Fig. 1, Cagliari *et al.* 2016, Valdez Buso *et al.* 2019, 2020). In this way, we can place the lower Rio Bonito Formation into Carboniferous, or we must assume that the upper fluvio-deltaic genetically related to the deep-marine deposits with glacial influence refers to Itararé Group, as employed by Aquino *et al.* (2016) and Valdez Buso *et al.* (2019) in the study area (Fig. 5). Thus, we argue that Rio Bonito Formation would correspond to the truly postglacial deposits developed above the upper fluvial-incised valley, dating Early Permian. Despite it, the development of the glacial or glacially influenced and postglacial deposits of Paraná Basin during the Late Paleozoic remains transitional in the Rio do Sul depocenter.

CONCLUSIONS

The registered stratigraphic framework reflects a complex paleogeographic scenario in the SW Gondwana during the deposition of the upper Itararé Group and the lower Rio Bonito Formation (Guatá Group), with a depocenter located in the region of Rio do Sul, Santa Catarina State, southern Brazil.

The examined succession comprises three evolutionary stages in which each depositional trend was recognized and traced in the subsurface, implying the regional expression of these events. Also, the stratigraphic stacking defined in the State of Santa Catarina reveals the presence of a glacial margin dynamic in the SW Gondwana, marked by cycles of advance and retreat. The first stage records a glacial advance from south-southwest configured by an erosional surface and the presence of subglacial tillites, whereas the gravitational deposits represent the ice retreat (upper Mafra Formation), and the following Lontras Shales is the marine maximum flooding. The

following stages point to a centripetal sediment feeding and glaciated source areas located NE, E, and SE. The least deglacial (Stage II) process of the Itararé Group is stratigraphically transitional to postglacial conditions of the Rio Bonito Formation, revealed by co-genetic glacially influenced deepwater to shallow deposits. The postglacial conditions were established in the third stage configured by the fill of the fluvial-incised valley, corresponding to upper Triunfo and Paraguaçu Members of the Rio Bonito Formation.

Features such as the fill pattern, thickness, and the transitional contact between Rio do Sul and Rio Bonito Formation establish the Rio do Sul depocenter. Besides the sea-level rising due to deglacial processes, it appears to be a tectonic overprinting on the eustatic signature creating space particularly recorded in the Rio do Sul depocenter. Likewise, the change of NW feeding

to the centripetal pattern points to the tectonic uplift of NE area during the upper Itararé instead of just the arm conditions of the uppermost Rio Bonito Formation as previously described.

ACKNOWLEDGMENTS

The Brazilian National Council for Scientific and Technological Development (CNPq, grant 461650/2014–2) funded this research. The authors thank the Coordination for the Improvement of Higher Education Personnel (CAPES) Foundation and the Human Resource Program of the Brazilian National Agency of Petroleum (PRH24-ANP) for the graduate scholarship to D. C. B. Schemiko and M. C. N. L. Rodrigues. Fernando Vesely has a CNPq fellowship. We thank Giorgio Basilici and Francisco M.W. Tognoli for comments and suggestions to improve the text.

ARTICLE INFORMATION

Manuscript ID: 20220027. Received on: 28 MAR 2022. Approved on: 5 AUG 2022.

How to cite this article: Schemiko D.C.B., Vesely F.F., Rodrigues M.C.N.L. Late Paleozoic glacial to postglacial stratigraphic evolution of the Rio do Sul depocenter, Itararé and Guatá groups, Pennsylvanian-Cisuralian, southern Brazil. *Brazilian Journal of Geology*, 52(4):e20220027, 2022. <https://doi.org/10.1590/2317-488920220220027>

D.C.B. Schemiko: Collected the data and interpreted them, wrote the manuscript, and prepared all the figures. F.F. Vesely: Collected data and provided guidance on the Late Paleozoic Ice Age of the Paraná Basin. M.C.N.L. Rodrigues: Provided data on mass transport deposits.

Competing interest: the authors declare no competing interests.

REFERENCES

- Amato J. 2017. *Using AMS to help interpret glaciogenic deposits of the Late Paleozoic ice age in the Paraná Basin, Brazil*. Master Thesis, University of Wisconsin, Milwaukee, 161 p.
- Aquino C.D., Valdez B.V., Faccini U.F., Milana J.P., Paim P.S.G. 2016. Facies and depositional architecture according to a jet efflux model of a late Paleozoic tidewater grounding line system from the Itararé Group (Paraná Basin), southern Brazil. *Journal of South American Earth Sciences*, 67:180-200. <https://doi.org/10.1016/j.jsames.2016.02.008>
- Bhattacharya J.P. 2006. Deltas. In: Posamentier H.W., Walker R.G. (Eds.). *Facies models revisited*. Oklahoma: Society for Sedimentary Geology, p. 237-292.
- Bhattacharya J.P. 2010. Deltas. In: James N., Dalrymple R. (Eds.). *Facies models*. Canada: Geological Association of Canada, p. 233-264.
- Blum M.D., Price D.M. 1998. Quaternary alluvial plain construction in response to glacio-eustatic and climatic controls, Texas Gulf Coastal Plain. In: Shanley K.W., McCabe P.J. (Eds.). *Relative role of eustasy climate and tectonism in continental rocks*. SEPM Special Publication, 59, p. 31-48.
- Bouma A.H. 1962. *Sedimentology of some flysh deposits, a graphic approach to facies interpretation*. Amsterdam: Elsevier, p. 168.
- Cagliari J., Lavina E.L.C., Philipp R.P., Tognoli F.M.W., Basei M.A.S., Faccini U.F. 2014. New Sakmarian ages for the Rio Bonito formation (Paraná Basin, southern Brazil) based on LA-ICP-MS U–Pb radiometric dating of zircons crystals. *Journal of South American Earth Sciences*, 56:265-277. <http://doi.org/10.1016/j.jsames.2014.09.013>
- Cagliari J., Philipp R.P., Valdez B.V., Netto R.G., Hillebrand P., Lopes C.R., Basei M.A.S., Faccini U.F. 2016. Age constraints of the glaciation in the Paraná Basin: evidence from new U–Pb dates. *Journal of the Geological Society*, 173(6):871-874. <https://doi.org/10.1144/jgs2015-161>
- Campos L., Milani E., Toledo M., Queiroz R., Catto A., Selke S. 1998. Barra Bonita: a primeira acumulação comercial de hidrocarboneto da Bacia do Paraná. In: Rio Oil & Gas Conference. *Anais...* Rio de Janeiro: Brazilian Petroleum Institute (IBP), p. 1-7.
- Canuto J.R. 1993. *Fácies e ambientes deposicionais da Formação Rio do Sul (Permiano), Bacia do Paraná, na região de Rio do Sul, Estado de Santa Catarina*. Thesis, Instituto de Geociências, Universidade de São Paulo, São Paulo, 183 p.
- Canuto J.R., Santos P.R., Rocha-Campos A.C. 2001. Estratigrafia de seqüências do Subgrupo Itararé (Neopaleozóico) no leste da Bacia do Paraná, nas regiões sul do Paraná e norte de Santa Catarina, Brasil. *Revista Brasileira de Geociências*, 31(1):107-116.
- Carvalho A.H., Vesely F.F. 2017. Facies relationship recorded in a Late Paleozoic fluvio-deltaic system (Parana Basin, Brazil): insights into the timing and triggers of subaqueous sediment gravity flows. *Sedimentary Geology*, 352:45-62. <https://doi.org/10.1016/j.sedgeo.2016.12.004>
- Castro J.C. 1980. *Fácies, ambientes e seqüências deposicionais das formações Rio do Sul e Rio Bonito, leste de Santa Catarina*. In: XXXI Congresso Brasileiro de Geologia. *Anais...* Camboriú, p. 283-299.
- Castro J.C. 1991. *A evolução dos sistemas glacial, marinho e deltaico das formações Rio do Sul e Rio Bonito/Mb. Triunfo (Eopermiano), sudeste da Bacia do Paraná*. Rio Claro. Thesis, Instituto de Geociências e Ciências Exatas, Universidade Estadual Paulista “Júlio de Mesquita Filho”, Rio Claro, 147 p.
- Castro J.C., Weinschütz L.C., Castro M.R. 2004. Estratigrafia de seqüências das Formações Taciba e Rio Bonito (Membro Triunfo) na região de Mafra/SC, leste da Bacia do Paraná. *Boletim de Geociências da Petrobras*, 13(1):27-42.
- Catuneanu O. 2006. *Principles of sequence stratigraphy*. Amsterdam: Elsevier, 375 p.
- Daemon R.F., Quadros L.P. 1970. Bioestratigrafia do Neopaleozoico da Bacia do Paraná. In: Congresso Brasileiro de Geologia, 24, 1970, Brasília. *Anais...* Brasília: SBG, 1, p. 359-412.
- D'Ávila R.S.F. 2009. *Seqüências deposicionais do Grupo Itararé (Carbonífero e Eopermiano), Bacia do Paraná, na área de Doutor Pedrinho e cercanias, Santa Catarina, Brasil: turbiditos, pelitos e depósitos caóticos*. Thesis, Unisinos, São Leopoldo, 245 p.
- D'Ávila R.S.F., Paim P.S.G. 2003. Mecanismos de transporte e deposição de turbiditos. In: Paim P.S.G., Faccini U.F., Netto R.G. (Eds.). *Geometria*,

- arquitetura e heterogeneidades de corpos sedimentares. São Leopoldo: Unisinos, p. 93-121.
- Evans D.J.A., Phillips E.R., Hiemstra J.F., Auton C.A. 2006. Subglacial till: formation, sedimentary characteristics and classification. *Earth-Science Reviews*, **78**(1-2):115-176. <https://doi.org/10.1016/j.earscirev.2006.04.001>
- Eyles N., Eyles C.H., França A.B. 1993. Glaciation and tectonics in an active intracratonic basin: The Late Paleozoic Itararé Group, Paraná Basin, Brazil. *Sedimentology*, **40**(1):1-25. <https://doi.org/10.1111/j.1365-3091.1993.tb01087.x>
- Eyles N., Eyles C.H., Miall A.D. 1983. Lithofacies types and vertical profile models: an alternative approach to the description and environmental interpretation of glacial diamictite and diamictite sequences. *Sedimentology*, **30**(3):393-410. <https://doi.org/10.1111/j.1365-3091.1983.tb00679.x>
- Fallgatter C., Paim P.S.G. 2017. On the origin of the Itararé group basal unconformity and its implications for the late Paleozoic glaciation in the Paraná Basin, Brazil. *Palaeogeography, Palaeoclimatology, Palaeoecology*, **531**(Part B):108225. <https://doi.org/10.1016/j.palaeo.2017.02.039>
- Fielding C.R., Frank T.D., Isbell J.L. 2008. Resolving the Late Paleozoic ice age intimate and space. *Geological Society of America Special Publication*, **441**:343-354.
- Flint R.F., Sanders J.E., Rodgers J. 1960. Diamictite, a substitute term for symmictite. *Geological Society of America Bulletin*, **71**(12):1809-1810. [https://doi.org/10.1130/0016-7606\(1960\)71\[1809:DASTFS\]2.0.CO;2](https://doi.org/10.1130/0016-7606(1960)71[1809:DASTFS]2.0.CO;2)
- França A.B., Potter P.E. 1988. Estratigrafia, ambiente deposicional e análise de reservatório do Grupo Itararé (Permocarboífero), Bacia do Paraná (parte 1). *Boletim de Geociências da Petrobras*, **2**:147-191.
- Gesicki A.L.D., Riccomini C., Boggiani P.C. 2002. Ice flow direction during the late Paleozoic glaciation in western Paraná Basin, Brazil. *Journal of South American Earth Sciences*, **14**(8):933-939. [https://doi.org/10.1016/S0895-9811\(01\)00076-1](https://doi.org/10.1016/S0895-9811(01)00076-1)
- Goodbred Jr. S.L., Kuehl S.A. 2000. The significance of large sediment supply, active tectonism, and eustasy on margin sequence development: Late Quaternary stratigraphy and evolution of the Ganges–Brahmaputra delta. *Sedimentary Geology*, **133**(3-4):227-248. [https://doi.org/10.1016/S0037-0738\(00\)00041-5](https://doi.org/10.1016/S0037-0738(00)00041-5)
- Goodbred Jr. S.L., Kuehl S.A., Steckler M.S., Sarker M.H. 2003. Controls on facies distribution and stratigraphic preservation in the Ganges–Brahmaputra delta sequence. *Sedimentary Geology*, **155**(3-4):301-316. [https://doi.org/10.1016/S0037-0738\(02\)00184-7](https://doi.org/10.1016/S0037-0738(02)00184-7)
- Griffis N.P., Montañez I.P., Mundil R., Le Heron R.D., Dietrich P., Kettler C., Linol B., Mottin T., Vesely F., Iannuzzi R., Huyskens M., Yin Q.-Z. 2021. High-latitude ice and climate control on sediment supply across SW Gondwana during the late Carboniferous and early Permian. *Geological Society of America Bulletin*, **133**(9-10):2113-2124. <https://doi.org/10.1130/B35852.1>
- Griffis N.P., Montañez I.P., Mundil R., Richey J., Isbell J., Fedorchuk N., Linol B., Iannuzzi R., Vesely F., Mottin T., Rosa E., Keller B., Yin Q.Z. 2019. Coupled stratigraphic and U-Pb zircon age constraints on the late Paleozoic icehouse-to-greenhouse turnover in south-central Gondwana. *Geology*, **47**(12):1146-1150. <https://doi.org/10.1130/G46740.1>
- Griffis N.P., Mundil R., Montañez I.P., Isbell J., Fedorchuk N., Vesely F., Iannuzzi R., Yin Q. 2018. A new stratigraphic framework built on U-Pb single-zircon TIMS ages and implications for the timing of the penultimate icehouse (Paraná Basin, Brazil). *The Geological Society of America Bulletin*, **130**(5-6):848-858. <https://doi.org/10.1130/B31775.1>
- Guerra-Sommer M., Cazzulo-Klepzig M., Menegat R., Formoso M.L.L., Basei M.A.S., Barboza E.G., Simas M.W. 2008a. Geochronological data from Faxinal coal succession in southern Paraná Basin: a preliminary approach combining radiometric U/Pb age and palynostratigraphy. *Journal of South American Earth Sciences*, **25**(2):246-256. <https://doi.org/10.1016/j.jsames.2007.06.007>
- Guerra-Sommer M., Cazzulo-Klepzig M., Santos J.O.S., Hartmann L.A., Ketzner J.M.M., Formoso M.L.L. 2008b. Radiometric age determination of tonsteins and stratigraphic constrains for the Lower Permian coal succession in southern Paraná Basin, Brazil. *International Journal of Coal Geology*, **74**(1):13-27. <https://doi.org/10.1016/j.coal.2007.09.005>
- Holz M., França A.B., Souza P.A., Iannuzzi R., Rohn R. 2010. A stratigraphic chart of the Late Carboniferous/Permian succession of the eastern border of the Paraná Basin, Brazil, South America. *Journal of South American Earth Science*, **29**(2):381-399. <https://doi.org/10.1016/j.jsames.2009.04.004>
- Holz M., Kuchle J., Philipp R.P., Bischoff A.P., Arima, N. 2006. Hierarchy of control on stratigraphic signatures: base-level changes during Early Permian in the Paraná Basin, southernmost Brazil. *Journal of South American Earth Sciences*, **22**(3-4):185-204. <https://doi.org/10.1016/j.jsames.2006.09.007>
- Hubbard S.M., Fildani A., Romans B.W., Covault J.A., McHargue T.R. 2010. High-relief slope clinoform development: insights from outcrop, Magallanes Basin, Chile. *Journal of Sedimentary Research*, **80**(5):357-375. <https://doi.org/10.2110/jsr.2010.042>
- Hunt D., Tucker M.E. 1992. Stranded parasequences and the forced regressive wedge systems tract: deposition during baselevel fall. *Sedimentary Geology*, **81**(1-2):1-9. [https://doi.org/10.1016/0037-0738\(92\)90052-S](https://doi.org/10.1016/0037-0738(92)90052-S)
- Iannuzzi R. 2010. The flora of Early Permian coal measures from the Paraná Basin in Brazil: a review. *International Journal of Coal Geology*, **83**(2-3):229-247. <https://doi.org/10.1016/j.coal.2010.05.009>
- Isbell J.L., Miller M.F., Wolfe K.L., Lenaker P.A. 2003. Timing of Late Paleozoic glaciation in Gondwana: Was glaciation responsible for the development of Northern Hemisphere cyclotherms? *Geological Society of America Special Papers*, **370**:5-24. <https://doi.org/10.1130/0-8137-2370-1-5>
- Kneller B.C., Branney M.J. 1995. Sustained high-density turbidity currents and the deposition of thick massive beds. *Sedimentology*, **42**(4):607-616. <https://doi.org/10.1111/j.1365-3091.1995.tb00395.x>
- Lima J.H.D., Netto R.G., Corrêa C.G., Lavina E.L.C. 2015. Ichnology of deglaciation deposits from the Upper Carboniferous Rio do Sul Formation (Itararé Group, Paraná Basin) at central-east Santa Catarina State (southern Brazil). *Journal of South American Earth Sciences*, **63**:137-148. <https://doi.org/10.1016/j.jsames.2015.07.008>
- López-Gamundí O.R., Buatois L.A. 2010. Introduction: Late Paleozoic glacial events and postglacial transgressions. In: López-Gamundí O.R., Buatois L.A. (Eds.), *Late paleozoic glacial events and postglacial transgressions in Gondwana*. Geological Society of America Special Paper, **468**:v-viii.
- Lowe D.R., Guy M. 2000. Slurry-low deposits in the Britannia Formation (Lower Cretaceous), North Sea: a new perspective on the turbidity current and debris flow problem. *Sedimentology*, **47**(1):31-70. <https://doi.org/10.1046/j.1365-3091.2000.00276.x>
- Matos S.L.F., Yamamoto J.K., Hachiro J., Coimbra A.M. 2000. Tonsteins da Formação Rio Bonito no depósito de carvão de candiota, RS. *Revista Brasileira de Geociências*, **30**(4):679-684. <https://doi.org/10.25249/0375-7536.2000304679684>
- Matos S.L.F., Yamamoto J.K., Riccomini C., Hachiro J., Tassinari C.C.G. 2001. Absolute dating of Permian ash-fall in the Rio Bonito Formation, Paraná Basin, Brazil. *Gondwana Research*, **4**(3):421-426. [https://doi.org/10.1016/S1342-937X\(05\)70341-5](https://doi.org/10.1016/S1342-937X(05)70341-5)
- Medeiros R.A., Thomaz Filho A. 1973. Facies e ambientes deposicionais da Formação Rio Bonito. XXVII Congresso Brasileiro de Geologia. *Anais...* Salvador, v. 3, p. 3-32.
- Miall A.D. 1978. Lithofacies types and vertical profile models of braided river deposits, a summary. In: Miall A.D. (Ed.). *Fluvial sedimentology*. Calgary: Canadian Society of Petroleum Geologists, p. 597-604.
- Miall A.D. 1996. *The geology of fluvial deposits: sedimentary facies, basin analysis and petroleum geology*. New York, Springer-Verlag, p. 582.
- Miall A.D. 2006. *The geology of fluvial deposits: sedimentary facies, basin analysis, and petroleum geology*. Berlin, Springer, pp. 582.
- Middleton G.V., Hampton M.A. 1973. Sediment gravity flows: mechanics of flow and deposition. In: Middleton G.V., Bouma A.H. (Eds.). *Turbidity and deep-water sedimentation*. Los Angeles: SEPM, p. 1-38.
- Milani E.J. 2004. Comentários sobre a origem e a evolução tectônica da Bacia do Paraná. In: Aatoria (Ed.). *Geologia do continente sul-americano*. São Paulo: editora, p. 266-279.
- Milani E.J., Melo J.H.G., Souza P.L., Fernandes L.A., França A.B. 2007. Bacia do Paraná. *Boletim de Geociências da Petrobras*, **1**:265-287.
- Milani E.J., Ramos V. 1998. Orogenias Paleozóicas no domínio sul-ocidental do Gondwana e os ciclos de subsidência da Bacia do Paraná. *Revista Brasileira de Geociências*, **28**(4):527-544.

- Mori A.L.O., Souza P.A., Marques J.C., Lopes R.C. 2012. A new U e Pb age dating and palynological data from a Lower Permian section of the southernmost Paraná a Basin, Brazil: biochronostratigraphical and geochronological implications for Gondwanan correlations. *Gondwana Research*, **21**(2-3):654-669. <https://doi.org/10.1016/j.jgr.2011.05.019>
- Mottin T.E., Vesely F.F. 2017. Controls on the Emplacement of Mass-Transport Diamictites in the Upper Itararé Group, Paraná Basin, Brazil. X Simpósio Sul-Brasileiro de Geologia. *Anais... Curitiba*, p. 1.
- Mottin T.E., Vesely F.F. 2021. Formação Taciba: última manifestação glacial no Paraná. *Boletim Paranaense de Geociências*, **78**:65-82. <https://doi.org/10.5380/geo.v78i0.79352>
- Mottin T.E., Vesely F.F., Lima Rodrigues M.C.N., Kipper F., Souza P.A. 2018. The paths and timing of late Paleozoic ice revisited: New stratigraphic and paleo-ice flow interpretations from a glacial succession in the upper Itararé Group (Paraná Basin, Brazil). *Palaeogeography, Palaeoclimatology, Palaeoecology*, **490**:488-504. <https://doi.org/10.1016/j.palaeo.2017.11.031>
- Mulder T., Alexander J. 2001. The physical character of sedimentary density currents and their deposits. *Sedimentology*, **48**(2):269-299. <https://doi.org/10.1046/j.1365-3091.2001.00360.x>
- Mulder T., Syvitski J.P.M., Migeon S., Faugères J.C., Savoye B. 2003. Marine hyperpycnal flows: initiation, behavior and related deposits. A review. *Marine and Petroleum Geology*, **20**(6-8):861-882. <https://doi.org/10.1016/j.marpetgeo.2003.01.003>
- Mutti E. 1962. *Turbidite sandstones*. Parma: AGIP and Università di Parma, 275 p.
- Mutti E., Davoli G., Tinterri R., Zavala C. 1996. The importance of ancient fluvio-deltaic systems dominated by catastrophic flooding in tectonically active basins. *Estratto da Memorie di Scienze Geologiche*, **48**:233-291.
- Neves J.P., Anelli L.E., Simões M.G. 2014. Early Permian post-glacial bivalve faunas of the Itararé Group, Parana Basin, Brazil: Paleocology and biocorrelations with South American intraplate basins. *Journal of South American Earth Sciences*, **52**:203-233. <https://doi.org/10.1016/j.jsames.2014.03.001>
- Noll S.H., Netto R.G. 2018. Microbially induced sedimentary structures in late Pennsylvanian glacial settings: A case study from the Gondwanan Paraná Basin. *Journal of South American Earth Sciences*, **88**:385-398. <https://doi.org/10.1016/j.jsames.2018.09.010>
- Northfleet A.A., Medeiros R.A., Mühlmann H. 1969. Reavaliação dos dados geológicos da Bacia do Paraná. *Boletim Técnico da Petrobras*, **12**:291-346.
- Popp J.H. 1983. Fácies, ambientes e carvões na Formação Rio Bonito no sul do Estado do Paraná: uma análise estratigráfica. *Revista Brasileira de Geociências*, **13**(1):27-36.
- Porebski S.J., Steel R.J. 2006. Deltas and sea-level change. *Journal of Sedimentary Research*, **76**(3):390-403. <https://doi.org/10.2110/jsr.2006.034>
- Puigdomenech C.N., Carvalho B., Paim P.S.G., Faccini U.F. 2014. Lowstand Turbidites and delta systems of the Itararé Group in the Vidal Ramos region (SC), southern Brazil. *Revista Brasileira de Geociências*, **44**(4):529-544. <https://doi.org/10.5327/Z23174889201400040002>
- Ramos A.N. 1967. Análise estratigráfica da Formação Rio Bonito. *Boletim Técnico da Petrobras*, **10**:307-407.
- Riccomini C., Almeida R.P., Turra B.B., Chamani M.A.C., Fairchild T.R., Hachiro J. 2005. Reativação de falha do embasamento causa sismicidade no Permian do Paraná. In: Simpósio Nacional de Estudos Tectônicos, **10**, 2005. *Boletim de Resumos Expandidos...*, p. 18-20.
- Rocha-Campos A.C., Machado L.C.R., Santos P.R., Canuto J.R., Castro J.C. 1988. Pavimento estriado da glaciação Neo-Paleozóica em Alfredo Wagner, SC, Brasil. *Boletim IG. Instituto de Geociências, USP*, **19**:39-46.
- Rocha-Campos A.C., Rössler O. 1978. Late Paleozoic faunal and floral successions in the Paraná Basin, southeastern Brazil. *Boletim IG. Instituto de Geociências, USP*, **9**:1-16.
- Rodrigues M.C.N.L., Trzaskos B., Alsop G.I., Vesely F.F., Mottin T.E., Schemiko D.C.B. 2021. Statistical analysis of structures commonly used to determine palaeoslopes from within mass transport deposits. *Journal of Structural Geology*, **151**:104421. <https://doi.org/10.1016/j.jsg.2021.104421>
- Rosa E.L.M., Vesely F.F., França A.B. 2016. A review on late Paleozoic ice-related erosional landforms of the Paraná Basin: origin and paleogeographical implications. *Brazilian Journal of Geology*, **46**(2):147-166. <https://doi.org/10.1590/2317-4889201620160050>
- Rosa E.L.M., Vesely F.F., Isbell J.L., Kipper F., Fedorchuk N.D., Souza P.A. 2019. Constraining the timing, kinematics and cyclicity of Mississippian-early Pennsylvanian glaciations in the Paraná Basin, Brazil. *Sedimentary Geology*, **384**:29-49. <https://doi.org/10.1016/j.sedgeo.2019.03.001>
- Rossi V.M., Steel R.J. 2016. The role of tidal, wave and river currents in the evolution of mixed-energy deltas: Example from the Lajas Formation (Argentina). *Sedimentology*, **63**(4):824-864. <https://doi.org/10.1111/sed.12240>
- Rostrirolla S.P., Assine M.L., Fernandes L.A., Artur P.C. 2000. Reativação de paleoalinhamentos durante a evolução da Bacia do Paraná - o exemplo do alto estrutural de Quatiguá. *Revista Brasileira de Geociências*, **30**(4):639-648.
- Santos P.R. 1987. Fácies e evolução paleogeográfica do Sub-Grupo Itararé/ Grupo Aquidauana (Neopaleozoico) na Bacia do Paraná, Brasil. Thesis, Instituto de Geociências, Universidade de São Paulo, São Paulo.
- Santos P.R., Rocha-Campos A.C., Canuto J.R. 1992. Estruturas de arrasto de ice-bergs em ritmitos do Subgrupo Itararé (Neo-Paleozóico), Trombudo Central, SC. *Boletim IG-USP. Série Científica*, **23**:1-18. <https://doi.org/10.11606/issn.2316-8986.v23i0p1-18>
- Santos P.R., Rocha-Campos A.C., Canuto J.R. 1996. Patterns of Late Paleozoic deglaciation in the Paraná Basin, Brazil. *Palaeogeography, Palaeoclimatology, Palaeoecology*, **125**(1-4):165-184. [https://doi.org/10.1016/S0031-0182\(96\)00029-6](https://doi.org/10.1016/S0031-0182(96)00029-6)
- Schemiko D.C.B., Vesely F.F., Rodrigues M.C.N.L., 2019. Deepwater to fluvio-deltaic stratigraphic evolution of a deglaciated depocenter: The early Permian Rio do Sul and Rio Bonito formations, southern Brazil. *Journal of South American Earth Sciences*, **95**:102260. <https://doi.org/10.1016/j.jsames.2019.102260>
- Schneider R.L., Mühlmann H., Tommasi E., Medeiros R.A., Daemon R.A., Nogueira A.A. 1974. Revisão estratigráfica da Bacia do Paraná. In: Congresso Brasileiro de Geologia, **27**, 1974. *Anais... Porto Alegre*, p. 41-65.
- Schoeneberger P.J., Wysocki D.A., Benham E.C., Soil Survey Staff. 2012. *Field book for describing and sampling soils, version 3.0*. Lincoln: Natural Resources Conservation Service, National Soil Survey Center, p. 9-14.
- Scomazzon A.K., Wilner E., Purnell M., Nascimento S., Weinschütz L.C., Lemos V.B., Souza F.L., Silva C.P. 2013. First report of conodont apparatuses from Brazil – Permian of Paraná Basin, Itararé Group, Lontras shale – Evidence of Gondwana Deglaciation. *Asociación Paleontológica Argentina, Publicación Especial*, (13):99-102.
- Shanmugam G. 2006. *Deep-water processes and facies models, implications for sandstone petroleum reservoirs*. Amsterdam: Elsevier, 476 p.
- Shanmugam G., Moiola R.J. 1988. Submarine fans: characteristics, models, classification, and reservoir potential. *Earth-Science Reviews*, **24**(6):383-428. [https://doi.org/10.1016/0012-8252\(88\)90064-5](https://doi.org/10.1016/0012-8252(88)90064-5)
- Shanmugam G., Wang Y. 2015. The landslide problem. *Journal of Palaeogeography*, **4**(2):109-166. <https://doi.org/10.3724/SPJ.1261.2015.00071>
- Silva D.C.D., Vega C.S., Vesely F.F., Schemiko D.C.B., Bolzon R.T. 2021. First occurrence of jumping trackway in upper Paleozoic glacially-related deposits, Paraná Basin, Brazil, and paleoenvironmental implications. *Ichnos*, **28**(4):259-270. <https://doi.org/10.1080/10420940.2021.1998036>
- Simões M.G., Neves J.P., Anelli L.E., Weinschutz L.C. 2012. Permian bivalves of the Taciba Formation, Itararé Group, Parana Basin, and their Biostratigraphic significance. *Geologia USP. Série Científica*, **12**(1):71-82. <https://doi.org/10.5327/Z1519-874X2012000100006>
- Souza P.A. 2006. Late Carboniferous palynostratigraphy of the Itararé Subgroup, northeastern Paraná Basin, Brazil. *Review of Paleobotany and Palynology*, **138**(1):9-29. <https://doi.org/10.1016/j.revpalbo.2005.09.004>
- Souza P.A., Boardman D.R., Premaor E., Félix C.M., Bender R.R., Oliveira E.J. 2021. The Vittatina costabilis Zone revisited: New characterization and implications on the Pennsylvanian-Permian icehouse-to-greenhouse turnover in the Paraná Basin, Western Gondwana. *Journal of South American Earth Sciences*, **106**:102968. <https://doi.org/10.1016/j.jsames.2020.102968>
- Souza P.A., Marques-Toigo M. 2005. Progress on the palynostratigraphy of the Permian strata in Rio Grande do Sul State, Paraná Basin, Brazil. *Anais da*

- Academia Brasileira de Ciências, 77(2):353-365. <https://doi.org/10.1590/S0001-37652005000200012>
- Souza P.A., Vesely F.F., Assine M.L. 1999. Contribuição palinológica ao conhecimento do Subgrupo Itararé na Serra dos Paes, sul do Estado de São Paulo. *Revista do Instituto Geológico*, 20(1-2):21-27. <https://doi.org/10.5935/0100-929X.19990002>
- Suss J.F., Vesely P.S.G., Catharina A.S., Assine M.L., Paim P.S.G. 2014. O Grupo Itararé (Neocarbonífero-Eopermiano) entre Porto Amazonas (PR) e Mafra (SC): Sedimentação gravitacional em contexto marinho deltaico sob a influência glacial. *Geociências*, 33(4):701-719.
- Tedesco J., Cagliari J., Aquino C.D. 2020. Late Paleozoic Ice-Age rhythmites in the southernmost Paraná Basin: A sedimentological and paleoenvironmental analysis. *Journal of Sedimentary Research*, 90(8):969-979. <https://doi.org/10.2110/jsr.2020.54>
- Thomas G.S.P., Connell R.J. 1985. Iceberg drop, dump and grounding structures from Pleistocene glaciolacustrine sediments, Scotland. *Journal of Sedimentary Research*, 55(2):243-249. <https://doi.org/10.1306/212F8689-2B24-11D7-8648000102C1865D>
- Tognoli F.M.W. 2006. *Estratigrafia das seqüências deposicionais do Grupo Guatá, borda leste da Bacia do Paraná*. Thesis, Instituto de Geociências e Ciências Exatas, Universidade Estadual Paulista "Júlio de Mesquita Filho", Rio Claro, 112 p.
- Tucker M.E. 2003. *Sedimentary rocks in the field*. Chichester: Wiley, 250 p. (The Geological Field Guide Series.)
- Valdez Buso V., Aquino C.D., Paim P.S.G., Souza P.A., Mori A.L., Fallgatter C., Milana J.P., Kneller B. 2019. Late Palaeozoic glacial cycles and subcycles in western Gondwana: correlation of surface and subsurface data of the Paraná Basin, Brazil. *Palaeogeography, Palaeoclimatology, Palaeoecology*, 531(Part B):108435. <https://doi.org/10.1016/j.palaeo.2017.09.004>
- Valdez Buso V., Milana J.P., di Pasquo M., Paim P.S.G., Philipp R.P., Aquino C.D., Cagliari J., Junior F.C., Kellner B. 2020. Timing of the Late Paleozoic glaciation in western Gondwana: New ages and correlations from Paganzo and Paraná Basins. *Palaeogeography, Palaeoclimatology, Palaeoecology*, 544:109-624. <https://doi.org/10.1016/j.palaeo.2020.109624>
- Vesely F.F. 2006. *Dinâmica sedimentar e arquitetura estratigráfica do Grupo Itararé (Carbonífero-Permiano) no centro-leste da Bacia do Paraná*. Thesis, Universidade Federal do Paraná, Curitiba, 226 p.
- Vesely F.F., Assine M.L. 2002. Superfícies estriadas em arenitos do Grupo Itararé produzidas por gelo flutuante, sudeste do Estado do Paraná. *Revista Brasileira Geociências*, 32(4):587-594.
- Vesely F.F., Assine M.L. 2006. Deglaciation sequences in the Permo-Carboniferous Itararé Group Paraná Basin, southern Brazil. *Journal of South American Earth Sciences*, 22(3-4):156-168. <https://doi.org/10.1016/j.jsames.2006.09.006>
- Vesely F.F., Trzaskos B., Kipper F., Assine M.L., Souza P.A. 2015. Sedimentary record of a fluctuating ice margin from the Pennsylvanian of western Gondwana: Paraná Basin, southern Brazil. *Sedimentary Geology*, 326:45-63. <https://doi.org/10.1016/j.sedgeo.2015.06.012>
- Visser J.N.J. 1990. Glacial bedforms at the base of the Permo-Carboniferous Dwyka Formation along the western margin of the Karoo Basin, South Africa. *Sedimentology*, 37(2):231-245. <https://doi.org/10.1111/j.1365-3091.1990.tb00957.x>
- Wilner E., Lemos V.B., Scomazzon A.K. 2016. Associações naturais de conodontes Mesogondolella spp., Grupo Itararé, Cisuraliano da Bacia do Paraná. *Gaea*, 9(1):30-36. <https://doi.org/10.4013/gaea.2016.91.02>
- Wilner E., Weinschütz L.C., Ricetti J.H.Z. 2012. Análise geoquímica do folhelho Lontras em Mafra, SC; Interpretações preliminares e constatações de sua fossildiagênese. *Boletim Informativo da Sociedade Brasileira de Paleontologia*, 66:107-108.
- Zacharias A.A., Assine M.L. 2005. Modelo de preenchimento de vales incisos por associações de fácies estuarinas, Formação Rio Bonito no norte do estado do Paraná. *Revista Brasileira de Geociências*, 35(4):573-583.
- Zavala C., Arcuri M., Di Meglio M., Gamero Diaz H., Contreras C. 2011. A genetic facies tract for the analysis of sustained hyperpycnal flow deposits. In: Slatt R.M., Zavala C. (Eds.). *Sediment transfer from shelf to deep water: revisiting the delivery system*. AAPG Studies in Geology, v. 61, p. 31-51.

Appendix 1. Localities described to construct this article.

Point	*UTM N	UTME	Ponto	*UTM N	UTME	Ponto	*UTM N	UTME
P01	633916	7012278	P67	631178	7025347	P131	636772	6997058
P02	631375	7013060	P68	634042	7021644	P132	634986	7002011
P03	631260	7013952	P69	635256	7017438	P133	637006	7007999
P04	629580	7014155	P70	639357	7009333	P134A	621821	6987126
P05	629387	7014252	P71	624994	7000181	P134B	621716	6987143
P06	631360	7013056	P72	626089	7004510	P134C	621685	6987154
P07	631504	7012713	P73	627937	7005696	P135	637497	6966622
P08	628459	7010114	P74	627656	7005642	P136	652579	6949654
P09	628388	7010254	P75	630413	7012936	P137	652852	6946895
P10	628273	7010348	P76	630540	7012308	P138	653200	6946461
P11	628137	7010417	P77	632846	7013633	P139	662917	6936470
P12	621227	7011964	P78	632583	7014523	P140	663466	6936152
P13	617126	6992299	P79	632885	7014705	P141	663469	6936155
P14	621070	6988660	P80	624206	7014079	P142	667104	6931297
P15	620919	6990104	P81	620802	7014027	P143	660302	6981909
P16	633558	6984887	P82	621911	7021368	P144	662512	6981708
P17	633460	6982421	P83	628164	7017979	P145	660776	6982674
P18	633690	6982103	P84	630730	7015941	P146A	660644	6982172
P19	637197	6973653	P85	634676	7040103	P146B	660581	6982220
P20	639644	6977009	P86	639003	7040057	P147	658191	6981775
P21	640161	6977059	P87	643701	7041137	P147B	658215	6981655
P22	635094	6971068	P88	639093	7018188	P148	658281	6982311
P23	637034	6968115	P89	639297	7017859	P149	663093	6970984
P24	638735	6965271	P90	639371	7017687	P150	660248	6968507
P25	665676	6976233	P91	639579	7017507	P151	659524	6967230
P26	663093	6977208	P92	638855	7018045	P151B	659870	6967378
P27	661415	6976834	P93	635214	7016887	P151C	659924	6967446
P28	661849	6979521	P94	640591	6998265	P152	657624	6969168
P29	670089	6975931	P95	640623	6998242	P153	656313	6967682
P30	662731	6970777	P96	641293	6998712	P154	657764	6968403
P31	662355	6970406	P97	641881	6998893	P155	657249	6967926
P32	662562	6969501	P98	642328	6998430	P156	654486	6970487
P33	662403	6969911	P99	642152	6999083	P157	660195	6968324
P34	662555	6969492	P100	629878	7013451	P158	664034	6966199
P35	650882	6954114	P101	630175	7013617	P159	663944	6966592
P36	672586	6942530	P102	630408	7012938	P160	663889	6966701
P37	672378	6942444	P103	630700	7012422	P161	664393	6966991
P38	672524	6942745	P104	626450	7020117	P162	663091	6967421
P39	672215	6943162	P105	625295	7022631	P163	662995	6967629
P40	666453	6935531	P106	625199	7021672	P164	662971	6967479
P41	662976	6935618	P107	641291	6994244	P165	662842	6967639
P42	662973	6935614	P108	638842	6997343	P166	665700	6976266
P43	675292	6936250	P109	636797	7006619	P167	665630	6976006
P44	675707	6937057	P110	641262	7003971	P168	665441	6975672
P45	672718	6932695	P111	641101	7003915	P169	665533	6975558
P46	686908	6936343	P112	640833	7003925	P170	665503	6975482
P47	636493	7008124	P113	640565	7003403	P171	665250	6975155
P48	631385	7013493	P114	637331	7004123	P172	652778	6981775
P49	620416	7021939	P115	636597	7003264	P173	662493	6969919
P50	616993	7022768	P116	627946	7005728	P174	662458	6969598
P51	615869	7024583	P117	626602	7000004	P175	662283	6969594
P52	616322	7024677	P118	633027	7006132	P176	661414	6968930
P53	615782	7025775	P119	632958	7006052	P179	663755	6970989
P54	631664	7004284	P120	633050	7005941	P180	663865	6970739
P55	632494	7004846	P121	633143	7005770	P181	664009	6970646
P56	616025	7027912	P122	633934	7005015	P182	663047	6970758
P57	633143	7005804	P123	633702	7004712	P183	662668	6971322
P58	632882	7006455	P124	633620	7004551	P184	656189	6969319
P59	631164	7007007	P125	633418	7004293	P185	656213	6969777
P60	633291	7006310	P126	630393	7002475	P186	656106	6969771
P61	630196	7007210	P127	629461	7002345	P187	663923	6961923
P62	633812	7004016	P128	629095	7002270	P188	619590	6981609
P63	625598	7012547	P129A	638637	6997393	P189	619743	6982103
P64	638018	7017425	P129C	638702	6997312	P190	619829	6981843
P65	640713	7020450	P129D	638768	6997303	P191	619241	6981157
P66	642646	7020821	P130	638472	6997564	P192	619576	6981405

*UTM SAD69; 22J.